"Interaction-free measurements of different absorbers"

by

Gerardo José Suárez Rodríguez

Submitted in Partial Fulfillment of the Requirements for the Degree
Master of Science,
Physics
Supervised by

Dr. Alonso Contreras Astorga
Dra. Sara Guadalupe Cruz y Cruz

16 April 2020

Declaration

I hereby certify that the material, which I now submit for assessment on the programmes of study leading to the award of Master of Science, is entirely my own work and has not been taken from the work of others except to the extent that such work has been cited and acknowledged within the text of my own work. No portion of the work contained in this thesis has been submitted in support of an application for another degree or qualification to this or any other institution.

_____

Gerardo Suárez

16 April 2020

Acknowledgements

Most figures were made using svgs from flaticom.com, the component library of Alexander Franzen and the noun project

List of Figures

List of Tables

Contents

Abstract

This is done at the end of the project

1 Introduction

1.1 al final

I am a subsection

1.1.1 Sub Subsection Example

I am a sub subsection

2   Preliminars

In this section we will develop the necessary tools to understand the rest of this thesis. We will start with the process by which we will generate single photons which we will use as input for our Mach-Zehnder interferometer. We then develop the theory of a lossless beam splitter, then we use this to explore both the classical and quantum Mach-Zehnder interferometers. In the case of the quantum version we explore different settings such as the Elitzur-Vaidman experiment and variations of it.

2.1   Spontaneous parametric down conversion

In this section we will explore the quantum theory of spontaneous parametric down conversion(SPDC), we will follow the approach taken in [1] and [2]. SPDC is a process where we make an intense laser beam go into a nonlinear crystal, occasionally one of the laser beam photons is annihilated and two photons of lower frequencies are created, Let us consider conservation of energy ($Energy_l = \hbar w_l$) where w is the angular frequency, and conservation on linear momentum ($\mathbf{p_l} = \hbar \mathbf{k_l}$) :

$$w_p = w_s + w_i \qquad \mathbf{k_p} = \mathbf{k}_s + \mathbf{k_i}, \tag{1}$$

Where the sub indices p, i, s refer to pump, signal and idler respectively. This is the name often used in the literature for each of the photons in the process. Pump refers to the photons of the laser beam. Signal to the one we wish to use and idler to another one we'll use just to know the other one was indeed a single photon(using entanglement).

There are three types of SPDC, which are known as type-0, type-I and type-II, respectively. The type of SPDC has to do with the polarization of each photon. In type-0 SPDC all photons have the same polarization.

In type-I both produced photons have the same polarization which is orthogonal to that of the pump. In this kind of SPDC both photons travel along the same

light-cone.

In the last type of SPDC, type-II both produced photons have orthogonal polarizations. In this type of SPDC each photon travels along it's own light-cone. In this thesis we are mainly concerned with the type-I SPDC process.

We will start our description of the SPDC process starting from the quantized electric field operator which can be written as:

$$\mathbf{E}(\mathbf{r},t) = \mathbf{E}^{(+)}(\mathbf{r},t) + \mathbf{E}^{(-)}(\mathbf{r},t), \tag{2}$$

$$\mathbf{E}^{(+)}(\mathbf{r},t) = \frac{1}{\sqrt{V}} \sum_{\mathbf{k},\nu} i(2\pi\hbar w)^{\frac{1}{2}} \hat{a}_{\mathbf{k},\nu} \hat{e}_{\mathbf{k},\nu} e^{i(\mathbf{k}.\mathbf{r}-wt)} = [\mathbf{E}^{(-)}(\mathbf{r},t)]^\dagger, \tag{3}$$

Where V is the quantization volume, $\hat{e}_{\mathbf{k},\nu}$ is the unit polarization vector orthogonal to the wave vector, for two polarizations $\nu = 1, 2$, and $\hat{a}_{\mathbf{k},\nu}$ is the photon annihilation operator.the expression is summed over all possible modes of the field. The ladder operators in this case follow the commutation relation:

$$[\hat{a}_{\mathbf{k},\nu}, \hat{a^\dagger}_{\mathbf{k},\nu}] = \delta_{\nu\nu'}\delta(\mathbf{k} - \mathbf{k'}). \tag{4}$$

The $\mathbf{E}^{(+)}(\mathbf{r},t)$ field operator acting on the vacuum state is:

$$\mathbf{E}^{(+)}(\mathbf{r},t)\ket{vacuum} = 0, \tag{5}$$

With the adjoint relation:

$$\bra{vacuum}\mathbf{E}^{(-)}(\mathbf{r},t) = 0. \tag{6}$$

Now, the Hamiltonian of an electromagnetic field can be written as:

$$H = \frac{1}{2}\int_V d^3r(\mathbf{D}\cdot\mathbf{E} + \mathbf{H}\cdot\mathbf{B}), \tag{7}$$

11

where $\mathbf{D}$ and $\mathbf{H}$ which are the electric displacement and the magnetic field respectively are given in terms of the electric field ($\mathbf{E}$) and the magnetic flux($\mathbf{B}$) by the constitutive equations(with ϵ_0 being the permittivity and and μ_0 the permeability of free space):

$$\mathbf{D} = \epsilon_0 \mathbf{E} + \mathbf{P}, \tag{8}$$

$$\mathbf{H} = \frac{\mathbf{B}}{\mu_0} - \mathbf{M}. \tag{9}$$

We will neglect $\mathbf{M}$ because we will assume that the laser beam is not strong enough to magnetize the crystal, so the Hamiltonian becomes:

$$H = \frac{1}{2} \int_V d^3r \left(\epsilon_0 \mathbf{E} \cdot \mathbf{E} + \mathbf{E} \cdot \mathbf{P} + \frac{\mathbf{B} \cdot \mathbf{B}}{\mu_0} \right) = H_0 + H_I. \tag{10}$$

The term H_I has to do with the interaction of the laser pump and the crystal, it is the one we will be studying. We will consider the polarization to be nonlinear and the linear term to be included in H_0, the main contributor to the process is the second order term in the nonlinear expansion (the expression for this second order polarization $P_i^{(2)}$ can be found in [3]):

$$H_I = \frac{1}{2} \int_V d^3r \, \mathbf{E}.\mathbf{P}^{(2)}, \tag{11}$$

$$P_i^{(2)} = \int_0^\infty dt_1 \int_0^\infty dt_2 \chi_{ijk}^{(2')}(t - t_1, t - t_2) E_j(\mathbf{r}, t_1) E_k(\mathbf{r}, t_2), \tag{12}$$

where $\chi_{ijk}^{(2')}$ is the second order nonlinear susceptibility, by substituting (12) in (11) and separating the fields in the creation and annihilation fields this can be written as:

$$H_I = \frac{1}{2} \int_V \int_0^\infty dt_1 \int_0^\infty dt_2 \chi_{ijk}^{(2')} (E_i^{(+)} E_j^{(+)} E_k^{(+)} + E_i^{(-)} E_j^{(+)} E_k^{(+)} + E_i^{(-)} E_j^{(-)} E_k^{(+)} +$$
$$E_i^{(+)} E_j^{(-)} E_k^{(+)} + E_i^{(+)} E_j^{(+)} E_k^{(-)} + E_i^{(-)} E_j^{(+)} E_k^{(-)} + E_i^{(-)} E_j^{(-)} E_k^{(-)} + E_i^{(+)} E_j^{(-)} E_k^{(-)}). \tag{13}$$

SPDC as we mentioned before is the annihilation of one photon and the creation of two. The only term compatible with this is $E_i^{(+)} E_j^{(-)} E_k^{(-)}$ as can be seen from equation (3), and its conjugate which means the reverse process. The other terms would not conserve energy so we do not consider them:

$$H_I = \int_V d^3 r \chi_{ijk}^{(2)} (E_i^{(+)} E_j^{(-)} E_k^{(-)} + H.C.), \tag{14}$$

where $H.C$ means hermitian conjugate and we redefined:

$$\chi_{ijk}^{(2)}(w_1, w_2) = \frac{1}{2} \int_0^\infty dt_1 \int_0^\infty dt_2 \chi_{ijk}(t_1, t_2)^{(2')}. \tag{15}$$

Replacing the expressions for the fields, and approximating the sum to an integral we take $\sum_{\mathbf{k}} \to \int d^3 k$

$$H_I = \int d^3 k_p \int d^3 k_s \int d^3 k_i \sum_{\nu_p, \nu_s, \nu_i} \chi_{ijk}^{(2)}(w_p, w_s, w_i)(\hat{e}_{k_p, \nu_p})_i (\hat{e}_{k_s, \nu_s})_j^\star (\hat{e}_{k_i, \nu_i})_k^\star \hat{a}_{\nu_p}(\mathbf{k_p}) \hat{a}^\dagger_{\nu_s}(\mathbf{k_s})$$
$$\hat{a}^\dagger_{\nu_i}(\mathbf{k_i}) e^{i(w_s + w_i - w_p)t} \int_V d^3 r e^{i\Delta \mathbf{k}.\mathbf{r}} + H.C,$$

where we defined:

$$\Delta \mathbf{k} = \mathbf{k_p} - \mathbf{k_s} - \mathbf{k_i}, \tag{16}$$
$$\chi_{ijk}^{(2)}(w_p, w_s, w_i) = \frac{-iV}{(2\pi)^9} (2\pi)^{\frac{3}{2}} (w_p w_s w_i)^{\frac{1}{2}} \chi_{ijk}^{(2)}. \tag{17}$$

Since polarizations are fixed in SPDC, we actually do not sum over ν but have a single value for it. Also we will consider $\chi_{ijk}^{(2)}$ to vary so slowly(in k and r) that we can treat it as a constant over the integrals. We will define $\chi = \chi_{ijk}^{(2)}(\hat{e}_{k_p,\nu_p})_i(\hat{e}_{k_s,\nu_s})_j^{\star}(\hat{e}_{k_i,\nu_i})_k^{\star}$ so we can write:

$$H_I = \chi \int d^3k_p \int d^3k_s \int d^3k_i \int_V d^3r \, \hat{a}_{\nu_p}(\mathbf{k_p})\hat{a}^{\dagger}_{\nu_s}(\mathbf{k_s})\hat{a}^{\dagger}_{\nu_i}(\mathbf{k_i})e^{i(w_s+w_i-w_p)t}e^{i\Delta\mathbf{k}.\mathbf{r}}+H.C. \tag{18}$$

Let us remember what the evolution operator definition is, let us use this to derive the Dyson series. Note that we will be using the H_I because we will be working in the interaction picture (since H_0 and H_I commute the interaction Hamiltonian is H_I):

$$U(t,t_0) = e^{\frac{1}{i\hbar}\int_{t_0}^t H_I(\tau)d\tau}, \tag{19}$$

$$|\psi(t)\rangle = U(t,t_0)|\psi(t_0)\rangle, \tag{20}$$

$$i\hbar\frac{d}{dt}|\psi(t)\rangle = H_I|\psi(t)\rangle, \tag{21}$$

$$i\hbar\frac{d}{dt}(U(t,t_0)|\psi(t_0)\rangle) = H_I(U(t,t_0)|\psi(t_0)\rangle). \tag{22}$$

By applying the Leibniz rule and because the equation must be valid for any ket, one can arrive to:

$$i\hbar\frac{d}{dt}U(t,t_0) = H_I U(t,t_0). \tag{23}$$

By direct integration, this can be written as an iterative integral equation, which is commonly known as Dyson series($U(t_0,t_0) = 1$):

$$U(t) = 1 - \frac{i}{\hbar}\int_{t_0}^t H_I(\tau)d\tau. \tag{24}$$

14

The laser beam or pump is in a coherent state [4]:

$$|\alpha\rangle = e^{\frac{-|\alpha|^2}{2}} \sum_{n=0}^{\infty} \frac{\alpha^n}{\sqrt{n!}} |n\rangle . \tag{25}$$

Coherent states are eigenstates of the annihilation operator with eigenvalue α which can be complex, it is known as the complex wave amplitude, this kind of state has the following properties:

$$\langle H \rangle = \hbar w(|\alpha|^2 + \frac{1}{2}), \qquad P_n = e^{-\langle n \rangle} \frac{\langle n \rangle^n}{n!}, \tag{26}$$

where P_n is the probability of finding n photons, it obeys poissonian statistics, our initial state is having the laser beam and no signal o idler photons that is a state $|\alpha_p, 0_s, 0_i\rangle$. Let us analyze the second order term of the Dyson series $U_1 = \frac{-i}{\hbar} \int_{t_0}^{t} H_I d\tau$ and apply it to the initial state:

$$U_1 |\psi(t_0)\rangle = \frac{-i\chi}{\hbar} \int_{-\infty}^{\infty} d\tau \int d^3 k_p \int d^3 k_s \int d^3 k_i \int d^3 r \alpha_p(\mathbf{k_p}, w_p) e^{i(w_s + w_i - w_p)t} e^{i\Delta \mathbf{k.r}} |\alpha_p, 1_s, 1_i\rangle , \tag{27}$$

in the last expression we already acted the ladder operators on the initial state that's why the $H.C$ does not appear since it annihilates the initial state. Integrating the exponential functions, our equation becomes:

$$U_1 |\psi(t_0)\rangle = \frac{-i\chi}{\hbar} (2\pi)^4 \int d^3 k_s \int d^3 k_i \alpha_p(\mathbf{k_s} + \mathbf{k_i}, w_p) \delta(w_s + w_i - w_p) |\alpha_p, 1_s, 1_i\rangle , \tag{28}$$

if we define $\xi = \frac{-i\chi(2\pi)^4}{\hbar} \int d^3 k_i \int d^3 k_s \delta(w_s + w_i - w_p) \delta(\mathbf{k_p} - \mathbf{k_s} - \mathbf{k_i})$ we can then rewrite in terms of operators as:

$$U_1 |\alpha_p, 0_s, 0_i\rangle = \xi \hat{a}_p \hat{a}_s^\dagger \hat{a}_i^\dagger |\alpha_p, 0_s, 0_i\rangle = \xi.\alpha_p |\alpha_p, 1_s, 1_i\rangle. \tag{29}$$

We will not consider higher orders, mainly for two reasons one that is that we are mainly interested in SPDC as single photon state generator (second order would generate 4 photons). And the second one is that higher orders are unlikely because the laser pump needs to be way more intense so that four photons would go out of the crystal at once.

2.2 First order joint amplitude function

Now that we've presented a quantum mechanical description of the phenomenon, we will use to generate single photon states. We are mainly concerned with the spatial correlations between the photons in the idler and signal channels, so we can know where we expect to detect them in our experiment as indicated by O.Rosas-Ortiz and L.M Procopio in [1]. We can find all information concerning the spatial correlations in the joint amplitude function which we aim to present in this section. Considering the last subsection our evolution operator can be written as:

$$U(t) = 1 + \xi \hat{a}_p \hat{a}_s^\dagger \hat{a}_i^\dagger. \tag{30}$$

So our state at any given time can be calculated by:

$$|\psi(t)\rangle = U(t,0) |\psi(t_0)\rangle, \tag{31}$$

$$|\psi(t)\rangle = |\alpha_p, 0_s, 0_i\rangle - \frac{-i\chi(2\pi)^4}{\hbar} \int d^3k_p \int d^3k_i \alpha_p(\mathbf{k_s} + \mathbf{k_i}, w_p)\delta(w_s + w_i - w_p) |\alpha_p, 1_s, 1_i\rangle. \tag{32}$$

We will rewrite this as:

16

$$|\psi(t)\rangle = |\alpha_p, 0_s, 0_i\rangle + \xi \int d^3k_s \int d^3k_i \Phi(\mathbf{k_i}, w_i, \mathbf{k_s}, w_s) |\alpha_p, 1_s, 1_i\rangle, \quad (33)$$

where we conveniently defined Φ:

$$\Phi(\mathbf{k_i}, w_i, \mathbf{k_s}, w_s) = \int d^3k_p \alpha_p(\mathbf{k_p}, w_p) \int_V d^3r e^{i\Delta\mathbf{k}.\mathbf{r}} \int d\tau e^{i(w_s + w_i - w_p)\tau}. \quad (34)$$

This Φ function is what is known in the current literature as the joint amplitude function, this one is first order because we stopped the Dyson series at first order. This function will enable us to study spatial correlations of the signal and idler channel in the next section.

2.3 Spatial correlations

Let us now study the spatial correlations from the joint amplitude function, to do this a couple approximations will be made. we start by rewriting it as:

$$\Phi(k_i, w_i, k_s, w_s) = \eta \alpha_p(\mathbf{k_s} + \mathbf{k_i}, w_p) \delta(w_p - w_s - w_i). \quad (35)$$

Let us assume α_p can be factorized into two functions, one that depends on the wave vectors and one that depends on the frequencies:

$$\Phi(k_i, w_i, k_s, w_s) = \eta G(\mathbf{k_i} + \mathbf{k_s}) F(w_p) \delta(w_p - w_s - w_i). \quad (36)$$

We will now separate the wave vectors into their transversal and longitudinal components:

$$\mathbf{k_r} = \mathbf{q_r} + k_{rz}\hat{e}_{rz}, \mathbf{q_r} = q_{rx}\hat{e}_{rx} + q_{ry}\hat{e}_{ry}, \quad (37)$$

where $r = p, s, i$. We will further assume paraxial beams, as Molina-Terriza and Minardi [5] demonstrated that in this situation the longitudinal components'

change with respect to the transversal are negligible. Let us assume that both functions G and F are Gaussian so that:

$$G(\mathbf{A}) = e^{-(\sigma|\mathbf{A}|)^2}, \qquad F(w)\delta(w - w') = e^{-(\delta w)^2}. \tag{38}$$

Using this we can rewrite the joint amplitude function as:

$$\Phi(\mathbf{q_i}, w_i, \mathbf{q_s}, w_s) = \eta e^{-\sigma^2|\mathbf{q_s}+\mathbf{q_i}|^2} F(w_s + w_i). \tag{39}$$

The spatial and spectral sensitivity of the detector are assumed to be given by Gaussian profile filters:

$$\mathbb{F}_s(\mathbf{q}_r) = e^{-|\sigma \cdot \mathbf{q}_r|^2}, \qquad \mathbb{F}_f(w_r) = e^{-(\alpha_r w_r)^2}. \tag{40}$$

Here $\sigma = (\sigma_{rx}, \sigma_{ry})$, and α_r, correspond to the spatial and frequency collection modes respectively, so we can write:

$$\Phi(\mathbf{q_i}, w_i, \mathbf{q_s}, w_s) = \Phi_f(w_i, w_s)\Phi_s(\mathbf{q_i}, \mathbf{q_s}). \tag{41}$$

That way separating it into to functions, one that tells us about the frequencies and the other one tells us about the spatial correlations:

$$\Phi_f(w_s, w_i) = \eta F_p(w_s + w_i)\mathbb{F}_f(w_i)\mathbb{F}_f(w_s), \tag{42}$$

$$\Phi_s(\mathbf{q_i}, \mathbf{q_s}) = e^{-\sigma^2|\mathbf{q_s}+\mathbf{q_i}|^2}\mathbb{F}_s(\mathbf{q_s})\mathbb{F}_s(\mathbf{q_i}). \tag{43}$$

Since we are in momentum space, we can obtain the spatial correlations by taking the Fourier transform:

$$\Phi_s(\mathbf{q_i}, \mathbf{q_s}) = \mathscr{F}(\Phi_s(\mathbf{q_i}, \mathbf{q_s})) = N \int d^2 q_i \int d^2 q_s \Phi_q(\mathbf{q_i}, \mathbf{q_s}) e^{-i\mathbf{q_s} \cdot \mathbf{r_s}} e^{-i\mathbf{q_i} \cdot \mathbf{r_i}}. \qquad (44)$$

This last equation encodes all spatial correlations between the signal and idler photon channels, allowing us to use this scheme to produce single photon states, by measuring in two positions which are highly correlated and only taking into account measurements where both detectors(one placed in the signal channel and the other in the idler channel) click, ensuring that this process took place and we indeed have single photon states.

2.4   The Mach-Zehnder interferometer

The Mach–Zehnder's flexibility in locating the fringes has made it the preferred interferometer for visualizing flow in wind tunnels [6] and for flow visualization studies in general. It is frequently used in several fields such as aerodynamics, plasma physics and heat transfer to measure pressure, density, and temperature changes in gases [7], they are used in electro-optic modulators [8], electronic devices used in various fiber-optic communication applications. Mach–Zehnder modulators are incorporated in monolithic integrated circuits and offer well-behaved [9], high-bandwidth electro-optic amplitude and phase responses over a multiple-gigahertz frequency range [10].

The Mach-Zehnder interferometer consists of two Beam Splitters (BS_1 and BS_2) and two mirrors (M_1 and M_2),two detectors D_1 and D_2 are placed in the output of the second beam splitter BS_2 as shown in Fig.1. The idea is to get an interference pattern from just one incoming beam which is then divided by BS_1 then it encounters a mirror in each path of the interferometer and it is then recombined in the second beam splitter its output is detected in either D_1 and D_2. We will now analyze the interferometer both in the classical and quantum regime.
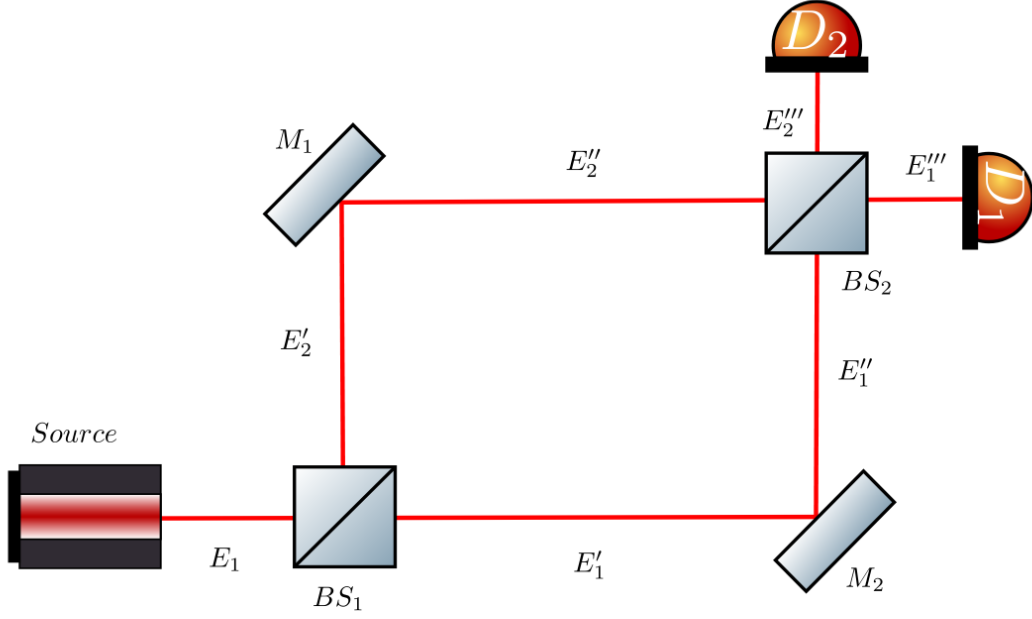
Figure 1: Mach Zehnder Interferometer

2.4.1 The classical and quantum beam splitter

This section is inspired in the beam splitter description presented in [11],[12] and [?], in this thesis we will consider ideal beam splitters which are reversible and lossless devices, this device has two inputs and two outputs, so two input beams may interfere to produce two outgoing beams. A beam splitter is usually a dielectric interface that is birefringent inside a cube as the Fig.2 shows:

The classical electric field can be written as:

$$\mathbf{E} = i\hat{\epsilon}Nw\left(\alpha e^{i(\mathbf{k}\cdot\mathbf{r}-wt)} + \alpha^* e^{i(\mathbf{k}\cdot\mathbf{r}-wt)}\right),\tag{45}$$

where α is known as the complex wave amplitude, to make our theoretical model of a beam splitter as general as possible, let us describe the device as a four-port
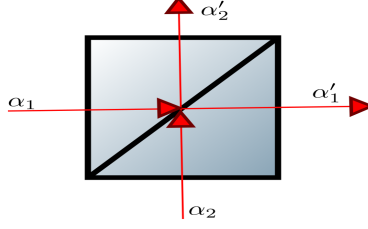
Figure 2: Beam splitter diagram

device, a black box with two input and two output ports having certain properties.

If two coherent light beams with complex wave amplitudes α_1 and α_2 enter the beam splitter, we simply expect the output complex wave amplitude are superimposed according to a linear transformation that we will call B so that:

$$\begin{pmatrix} \alpha_1' \\ \alpha_2' \end{pmatrix} = B \begin{pmatrix} \alpha_1 \\ \alpha_2 \end{pmatrix}. \tag{46}$$

The linear transformation B is described by a matrix:

$$B = \begin{pmatrix} B_{11} & B_{12} \\ B_{21} & B_{22} \end{pmatrix}. \tag{47}$$

Since the beam splitter is a lossless device and it does not amplify the fields we want B to be a unitary transformation, so it needs to fulfill the following relationship

$$|B_{11}|^2 + |B_{12}|^2 = |B_{21}|^2 + |B_{22}|^2 = 1, \qquad B_{11}B_{21}^* + B_{12}B_{22}^* = 0. \tag{48}$$

We will write this matrix in terms of the reflectivity ρ and the transmissivity τ that follow the relationship:

$$|\tau|^2 + |\rho|^2 = 1. \tag{49}$$

In the classical case the transformation is usually written as:

$$B = \begin{pmatrix} \tau & \rho \\ -\rho & \tau \end{pmatrix}.$$

(50)

so that

$$\begin{pmatrix} E_1' \\ E_2' \end{pmatrix} = \begin{pmatrix} \tau & \rho \\ -\rho & \tau \end{pmatrix} \begin{pmatrix} E_1 \\ E_2 \end{pmatrix}.$$

(51)

While in the classical case what happens is that the complex wave amplitudes are promoted to annihilation and creation operators as was explained in the SPDC section, in the quantum case the B matrix is usually written as:

$$B = \begin{pmatrix} \cos(\theta) & i\sin(\theta) \\ i\sin(\theta) & \cos(\theta) \end{pmatrix}.$$

(52)

Instead of the fields it is customary to write the linear transformation in terms of the ladder operators so that:

$$\begin{pmatrix} a_1' \\ a_2' \end{pmatrix} = \begin{pmatrix} \cos(\theta) & i\sin(\theta) \\ i\sin(\theta) & \cos(\theta) \end{pmatrix} \begin{pmatrix} a_1 \\ a_2 \end{pmatrix}$$

(53)

In the quantum case we are just interested in the single photon state, which we can now explore, to begin our analysis of the quantum version it is necessary to decide in which basis we want to work in order to represent our operators, we will work in the Horizontal-Vertical basis. Let us denote:

$$|1\rangle = |1\rangle_h \, |0\rangle_v = \begin{pmatrix} 1 \\ 0 \end{pmatrix},$$

(54)

the state of the field with one photon in the horizontal path and zero in the vertical path

$$|2\rangle = |0\rangle_h \, |1\rangle_v = \begin{pmatrix} 0 \\ 1 \end{pmatrix}, \tag{55}$$

the state with 0 photons in the horizontal path and 1one in the vertical path. A mirror in the subspace span $(|1\rangle, |2\rangle)$ simply flips the state and adds a phase:

$$M = \begin{pmatrix} 0 & e^{i\gamma} \\ e^{i\gamma} & 0 \end{pmatrix}. \tag{56}$$

We have now defined all the things we need in order to analyze the interferometer in the classical and quantum case. Which we will do in the next sections.

2.4.2 Classical Mach-Zehnder

In this section we study the Mach-Zehnder interferometer in the classical regime. We will denote the classical fields going through the interferometer as is shown in Fig.1. We will follow the approach taken by Loudon [?]. Let us consider two lossless beam splitters $BS_1 = BS_2$. The electric field E_1 of the incident beam is then splitted as:

$$E_1' = \tau E_1, \qquad E_2' = \rho E_1. \tag{57}$$

The mirrors described by the matrix M only add a phase $e^{i\phi_i}$, where $i = 1, 2$. We can proceed to calculate the intensity of the fields in the output

$$E_1'' = e^{ik\phi_1} E_1', \qquad E_2'' = e^{ik\phi_2} E_2'. \tag{58}$$

Then those fields go through the second BS:

$$E_1''' = \tau E_2'' + \rho E_1'', \qquad E_2''' = \tau E_1'' - \rho E_2''. \tag{59}$$

Substituting the expressions obtained before the above equations can be written as :

$$E_1''' = \tau\rho(e^{ik\phi_1} + e^{ik\phi_2})E_1.$$
$$E_2''' = \tau^2 e^{ik\phi_1}E_1 - \rho^2 e^{ik\phi_2}E_1. \tag{60}$$

We can calculate intensities at the detectors by taking the modulus squared of the fields, we use $\delta\phi = \phi_1 - \phi_2$:

$$I_{D1} \propto |E_1|^2 2(\rho\tau)^2(1 + \cos(k\delta\phi)).$$
$$I_{D2} \propto |E_1|^2(\rho^4 + \tau^4)(1 - \frac{2(\rho\tau)^2}{\rho^4 + \tau^4}\cos(k\delta\phi)). \tag{61}$$

A case of interest is when $\rho = \tau = \frac{1}{\sqrt{2}}$, then the intensities become:

$$I_{D1} \propto |E_1|^2 \frac{1 + \cos(k\delta\phi)}{2}.$$
$$I_{D2} \propto |E_1|^2 \frac{1 - \cos(k\delta\phi)}{2}. \tag{62}$$

When $\delta\phi = \lambda n$ where $n = 1, 2, 3, ...$, so $\cos(2\pi n) = 1$ and the detector D_1 receives the intensity of the initial beam and D_2 receives no light.

$$I_{D1} \propto |E_1|^2, \qquad I_{D2} \propto 0. \tag{63}$$

2.4.3 Single photon Mach-Zehnder

In this section we will study a single photon Mach-Zehnder, which will be the main object of concern in the rest of this thesis. for this part of the analysis we will assume mirrors that induce different phases in each path. This is done to analyze misalignment and as proven later is equivalent to considering phase-shifters inducing differences in the optical paths.

$$M_i = \begin{pmatrix} 0 & e^{i\gamma_i} \\ e^{i\gamma_i} & 0 \end{pmatrix}. \tag{64}$$

Once we have defined the main elements we can analyze the single photon Mach-Zehnder interferometer. A single photon is generated via SPDC and is sent in the horizontal path of the interferometer as input, so $|1\rangle$ is our initial state which encounters the first BS

$$|1\rangle \xrightarrow{\text{BS}} \cos(\theta)\,|1\rangle + i\sin(\theta)\,|2\rangle. \tag{65}$$

To study a general situation, we will consider two different BS in our interferometer. Note that the action of optical elements is local. After the first BS, the photon encounters a mirror in each path, and then both paths are recombined in the second BS. The whole action of the interferometer on the initial state $|1\rangle$ is then:

$$|1\rangle \xrightarrow{\text{BS1}} \cos(\theta_1)\,|1\rangle + i\sin(\theta_1)\,|2\rangle \xrightarrow{\text{Mirrors}} \cos(\theta_1)e^{i\gamma_1}\,|2\rangle + i\sin(\theta_1)e^{i\gamma_2}\,|1\rangle$$
$$\xrightarrow{\text{BS2}} i(\cos(\theta_1)\sin(\theta_2)e^{i\gamma_1} + \cos(\theta_2)\sin(\theta_1)e^{i\gamma_2})\,|1\rangle +$$
$$(\cos(\theta_1)\cos(\theta_2)e^{i\gamma_1} - \sin(\theta_1)\sin(\theta_2)e^{i\gamma_2})\,|2\rangle. \tag{66}$$

To compare with the classical case where we did our calculations with two identical

BS we make $\theta_1 = \theta_2 = \frac{\pi}{4}$ then the state at the output of the interferometer is

$$|\psi\rangle = \frac{i}{2}(e^{i\gamma_1} + e^{i\gamma_2})|1\rangle + \frac{1}{2}(e^{i\gamma_1} - e^{i\gamma_2})|2\rangle$$

$$|\psi\rangle = \frac{e^{i(\gamma_1 + \frac{\pi}{2})}}{2}(1 + e^{i(\gamma_2 - \gamma_1)})|1\rangle + \frac{e^{i\gamma_1}}{2}(1 - e^{i(\gamma_2 - \gamma_1)})|2\rangle \qquad (67)$$

To obtain the probabilities at the output we simply compute:

$$P_{D_1} = |\langle 1|\psi\rangle|^2, \qquad\qquad P_{D_2} = |\langle 2|\psi\rangle|^2 \qquad (68)$$

$$P_{D_1} = \frac{1 + \cos(\gamma_2 - \gamma_1)}{2}, \qquad\qquad P_{D_2} = \frac{1 - \cos(\gamma_2 - \gamma_1)}{2} \qquad (69)$$

Perfect alignment means no difference in the optical path so that $\gamma_2 - \gamma_1 = 0$, then the probability to detect in D_1 is one and in D_2 is zero, perfectly compatible with the result obtained in the classical case, we expect a similar result because the classical case is basically many repetitions of this case.

2.4.4 Single photon Mach-Zehnder interferometer with a perfect absorber

This case is best known as the Elitzur-Vaidman's bomb detector [13], an interesting aspect of this experiment is that it shows a little of the non-local nature of quantum mechanics, by getting knowledge of whether a "bomb" (perfect absorber) is in one of the arms of the interferometer by measuring a photon that did not interact with the "bomb" (if it did it would be absorbed). The bomb is supposed to explode if a single photon interacts with it, the proposal of Elitzur and Vaidman was to have a mechanism such that one could detect if the bomb was there or not, without it exploding. Our calculations will show that this can be achieved about 50% of the time at most.

To analyze this case we will simply repeat the calculations we did above this time having a perfect absorber in the vertical arm of the interferometer as the Fig. 2
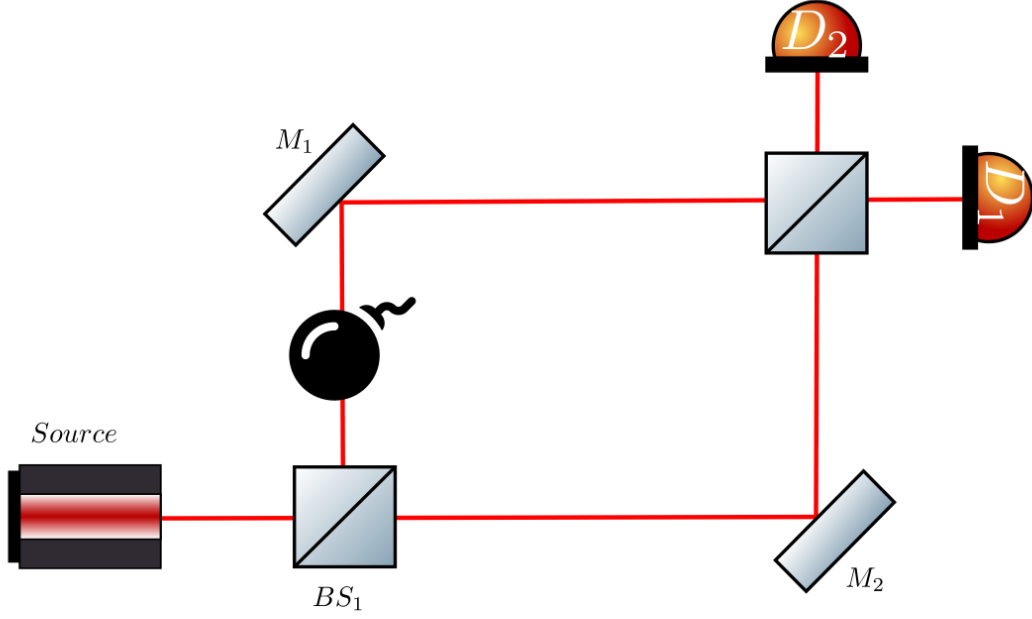
Figure 3: Elitzur-Vaidman's bomb detector

shows. We also need to consider that once the photon is absorbed the optical elements do not interact with it anymore. We will denote an absorbed photon using the $|Abs\rangle$ state. First the initial state is transformed by the first BS then the , vertical path is absorbed by our perfect absorber then the state encounters mirrors and then if finally recombined in the second BS

$$|1\rangle \xrightarrow{\text{BS1}} \cos(\theta_1)|1\rangle + i\sin(\theta_1)|2\rangle$$
$$\xrightarrow{\text{Bomb}} \cos(\theta_1)|1\rangle + i\sin(\theta_1)|Abs\rangle$$
$$\xrightarrow{\text{Mirrors}} i\cos(\theta_1)|2\rangle + i\sin(\theta_1)|Abs\rangle$$
$$\xrightarrow{\text{BS2}} i\cos(\theta_1)\cos(\theta_2)|2\rangle - \cos(\theta_1)\sin(\theta_2)|1\rangle + i\sin(\theta_1)|Abs\rangle \qquad (70)$$

The probabilities to be absorbed or detected at either D_1 or D_2 are given by :

$$P_{D1} = \cos^2(\theta_1)\sin^2(\theta_2). \tag{71}$$

$$P_{D2} = \cos^2(\theta_1)\cos^2(\theta_2). \tag{72}$$

$$P_{Abs} = \sin^2(\theta_1). \tag{73}$$

Let us again consider the case where $\theta_1 = \theta_2 = \frac{\pi}{4}$ then:

$$P_{D1} = \frac{1}{4}, \quad P_{D2} = \frac{1}{4}, \quad P_{Abs} = \frac{1}{2}. \tag{74}$$

If the photon is detected at D_2 it would indicate that there's an object in one of the arms of the interferometer. This is often called non-interactive measurements because we can infer information of the object from the photons that did not interact with it. We cannot really distinguish between this case and the previous one from a single event if we detect at D_1, so $\frac{1}{2}$ of the times we make a measurement we can't really tell if a bomb is there or not.

2.4.5 The single photon Mach-Zehnder interferometer with an imperfect transmitter

This section and the next ones are based on the treatment done by Z.Blanco and O.Rosas-Ortiz [14] [15] and the work done by Azuma [16]. Let us consider an object such that α' and β' are its absorption and transmission coefficients, respectively, satisfying the condition $|\alpha|^2 + |\beta|^2 = 1$..

We will use the same Horizontal-Vertical basis and our initial state $|1\rangle$. We will place our imperfect absorber in the vertical path. Our absorber can either transmit with probability $|\beta|^2$ or absorb with probability $|\alpha|^2$, such that when encountered with this object our states become:

28

$$|2\rangle \xrightarrow[\text{Absorber}]{\text{Imperfect}} \alpha \,|abs\rangle + \beta \,|2\rangle. \tag{75}$$

With this information we can now go on with our calculations, First the initial state goes through a BS, then it encounters our imperfect transmitter, after that it goes through a mirror in each path and then it is finally recombined in the second BS:

$$
\begin{aligned}
|1\rangle \xrightarrow{\text{BS1}} & \cos(\theta_1)\,|1\rangle + i\sin(\theta_1)\,|2\rangle \\
\xrightarrow[\text{Absorber}]{\text{Imperfect}} & \cos(\theta_1)\,|1\rangle + i\sin(\theta_1)(\alpha\,|abs\rangle + \beta\,|2\rangle) \\
\xrightarrow{\text{Mirrors}} & i\cos(\theta_1)\,|2\rangle + i\sin(\theta_1)\alpha\,|abs\rangle - \sin(\theta_1)\beta\,|1\rangle \\
\xrightarrow{\text{BS2}} & -(\cos(\theta_1)\sin(\theta_2) + \beta\sin(\theta_1)\cos(\theta_2))\,|1\rangle + i\alpha\sin(\theta_1)\,|abs\rangle + \\
& i(\cos(\theta_1)\cos(\theta_2) - \sin(\theta_1)\sin(\theta_2)\beta)\,|2\rangle.
\end{aligned} \tag{76}
$$

We will write detection probabilities as P_{ij} where $i = 1, 2$ the path of the interferometer where the imperfect transmitter is placed, and j is one of the possible outcomes, therefore the detection probabilities are given by:

$$P_{2D1} = |\cos(\theta_1)\sin(\theta_2) + \beta\sin(\theta_1)\cos(\theta_2)|^2. \tag{77}$$

$$P_{2D2} = |\cos(\theta_1)\cos(\theta_2) - \beta\sin(\theta_1)\sin(\theta_2)|^2. \tag{78}$$

$$P_{2abs} = |\alpha\sin(\theta_1)|^2. \tag{79}$$

If we consider the exact same procedure but this time we put our imperfect absorber on the horizontal arm of the interferometer we obtain:

$$P_{1D1} = |\cos(\theta_1)\sin(\theta_2)\beta + \sin(\theta_1)\cos(\theta_2)|^2. \tag{80}$$

$$P_{1D2} = |\sin(\theta_1)\sin(\theta_2) - \beta\cos(\theta_1)\cos(\theta_2)|^2. \tag{81}$$

$$P_{1abs} = |\alpha\cos(\theta_1)|^2. \tag{82}$$

Observing the probabilities are different we can obtain the difference between them, expressions concerning the difference between PD_1 and PD_2 are important because they tell us just how distinguishable these outcomes are:

$$P_{1D1} - P_{1D2} = (1 - |\beta|^2)\left(\frac{\cos(2\theta_1) - \cos(2\theta_2)}{2}\right). \tag{83}$$

$$P_{2D1} - P_{2D2} = (1 - |\beta|^2)\left(\frac{\cos(2\theta_1) + \cos(2\theta_2)}{2}\right). \tag{84}$$

From there, we can say that the probabilities are the same only when :

a)$\beta = 1$ which means a transparent object.

b)$\cos(2\theta_2) + \cos(2\theta_1) = \cos(2\theta_1) - \cos(2\theta_2) = 0$ which means $\theta_1 = \theta_2 = \frac{\pi}{4} \pm 2n\pi$.

We can also obtain an expression for one of the angles in terms of the probabilities

$$\theta_2 = \frac{\cos^{-1}[(P_{1D2} - P_{1D1}) - (P_{1D1} - P_{2D1})]}{2}. \tag{85}$$

$$\theta_1 = \frac{\cos^{-1}[(P_{1D2} - P_{1D1}) + (P_{1D1} - P_{2D1})]}{2}. \tag{86}$$

3 Mach-Zenhder interferometer with a beam splitter as imperfect trasmitter

We will now study the case of a BS as an imperfect transmitter. We consider imperfect mirrors such that $\gamma \neq 0$. We will see this is equivalent to including phase shifters in section 3.2, like in the previous cases we will first consider our imperfect transmitter in the vertical path as the Fig.4 shows, as we can see from the figure the reflected photon goes out of the interferometer's paths and therefore it's lost instead of being absorbed.
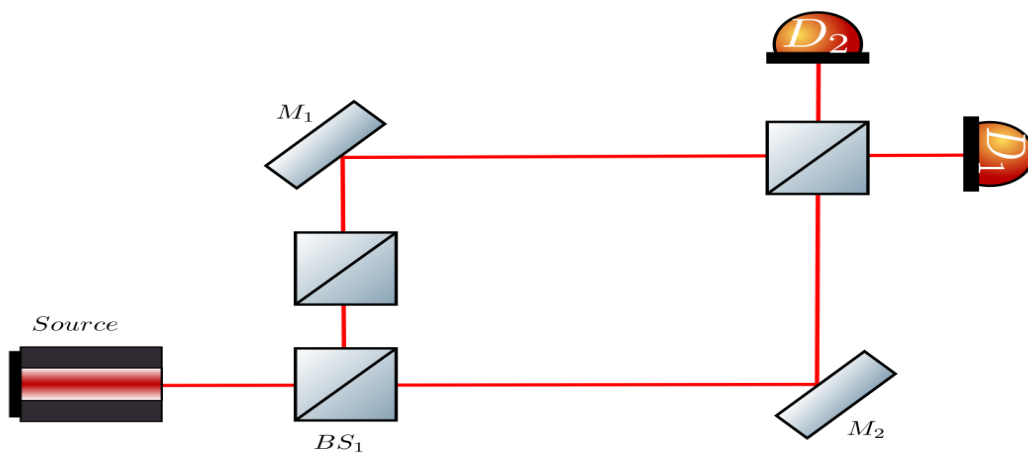
Figure 4: Mach-Zehnder interferometer with a BS as imperfect transmitter

Our imperfect transmitter is a BS whose transmission coefficient is $\cos(\theta_o)$ and its reflection coefficient is $i\sin(\theta_o)$. When a state interacts with our imperfect transmitter it becomes:

$$|2\rangle \xrightarrow[\text{Absorber}]{\text{Imperfect}} i\sin(\theta_o)\,|abs\rangle + \cos(\theta_o)\,|2\rangle. \tag{87}$$

We consider the reflected photon to be lost since it goes out of our interferometer,

(a) P_{2Abs}

(b) P_{2D1}

(c) P_{2D2}

Figure 5: Probability distributions with imperfect absorber in vertical path and $\theta_o = \frac{\pi}{3}$ y $\gamma_2 - \gamma_1 = \pi$.

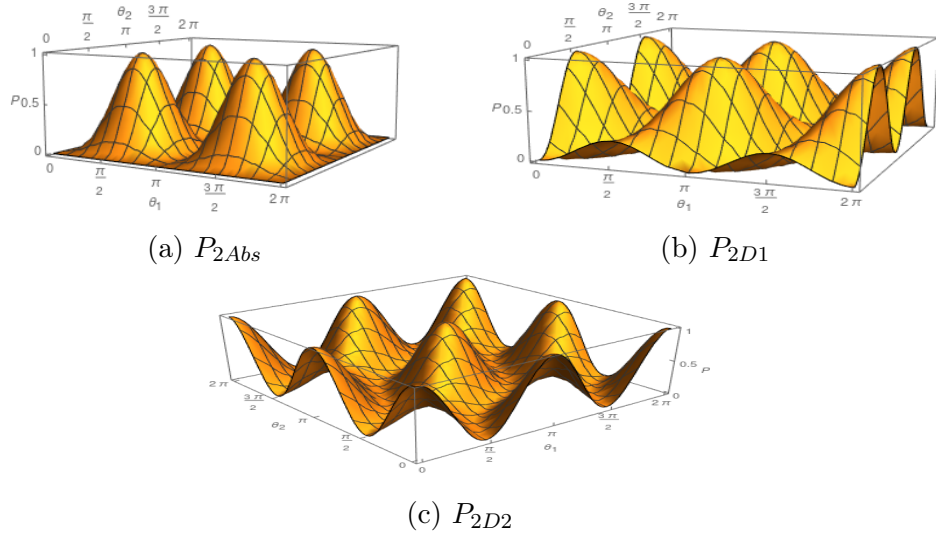and we denote that "lost photon" state by $|abs\rangle$, with that in mind now we can begin our calculation which is analogous to the ones from the previous sections:

$$|1\rangle \xrightarrow{\text{BS1}} \cos(\theta_1)|1\rangle + i\sin(\theta_1)|2\rangle \xrightarrow{\text{BS}} \cos(\theta_1)|1\rangle + i\sin(\theta_1)(\cos(\theta_o)|2\rangle + i\sin(\theta_o)|abs\rangle)$$

$$\xrightarrow{\text{Mirrors}} \cos(\theta_1)e^{i\gamma_1}|2\rangle + i\sin(\theta_1)\cos(\theta_o)e^{i\gamma_2}|1\rangle - \sin(\theta_1)\sin(\theta_o)|abs\rangle$$

$$\xrightarrow{\text{BS2}} \cos(\theta_1)e^{i\gamma_1}(\cos(\theta_2)|2\rangle + i\sin(\theta_2)|1\rangle) + i\sin(\theta_1)\cos(\theta_o)e^{i\gamma_2}(\cos(\theta_2)|1\rangle + i\sin(\theta_2)|2\rangle) -$$

$$\sin(\theta_1)\sin(\theta_o)|abs\rangle$$

$$= (\cos(\theta_1)e^{i\gamma_1}\cos(\theta_2) - \sin(\theta_1)\sin(\theta_2)\cos(\theta_o)e^{i\gamma_2})|2\rangle - \sin(\theta_1)\sin(\theta_o)|abs\rangle + (i\cos(\theta_1)\sin(\theta_2)e^{i\gamma_1} +$$

$$i\sin(\theta_1)\cos(\theta_o)\cos(\theta_2)e^{i\gamma_2})|1\rangle. \tag{88}$$

Detection probabilities are shown in Fig.5, where we can see that for certain values of θ_i where $i = 1, 2, o$ the probabilities of detection in D_2 can be really close to one:

32

(a) P_{1Abs}

(b) P_{1D1}

(c) P_{1D1}
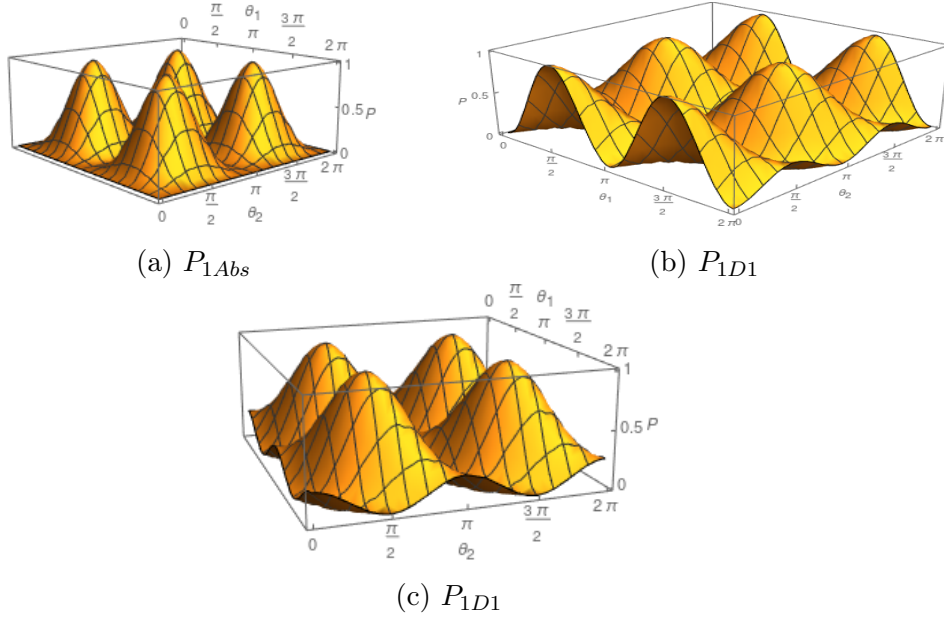
Figure 6: Probabilities distribution in the Horizontal path for $\theta_o = \frac{\pi}{3}$ y $\gamma_2 - \gamma_1 = \pi$

$$P_{2D1} = |ie^{i\gamma_1} \cos(\theta_1) \sin(\theta_2) + ie^{i\gamma_2} \cos(\theta_o) \sin(\theta_1) \cos(\theta_2)|^2. \tag{89}$$

$$P_{2D2} = |\cos(\theta_1) \cos(\theta_2) e^{i\gamma_1} - e^{i\gamma_2} \cos(\theta_o) \sin(\theta_1) \sin(\theta_2)|^2. \tag{90}$$

$$P_{2Abs} = |\sin(\theta_o) \sin(\theta_1)|^2. \tag{91}$$

Repeating the exact same calculation with the object in the horizontal path we obtain the following probabilities, which are shown graphically in Fig.6. We can see they are quite different and that is because we are always launching our photon from the same path therefore the situation is not symmetrical, that is the object isn't always in the same path the photon was sent into:

$$P_{1D1} = |ie^{i\gamma_1}\cos(\theta_1)\sin(\theta_2)\cos(\theta_o) + ie^{i\gamma_2}\sin(\theta_1)\cos(\theta_2)|^2. \tag{92}$$

$$P_{1D2} = |\cos(\theta_1)\cos(\theta_o)\cos(\theta_2)e^{i\gamma_1} - e^{i\gamma_2}\sin(\theta_1)\sin(\theta_2)|^2. \tag{93}$$

$$P_{1Abs} = |\sin(\theta_o)\cos(\theta_1)|^2. \tag{94}$$

This analysis is totally consistent with Zurika's [14] when one takes the case $\beta' = \cos(\theta_o)$, $\alpha' = i\sin(\theta_o)$ and $\gamma_2 - \gamma_1 = 0$. However this case has a little advantage and that is that our "absorbed" photon, is not absorbed but goes out of our interferometer so we can actually measure all outputs of the interferometer by placing a detector, say D_{abs}, in the path the "lost photon" would follow.
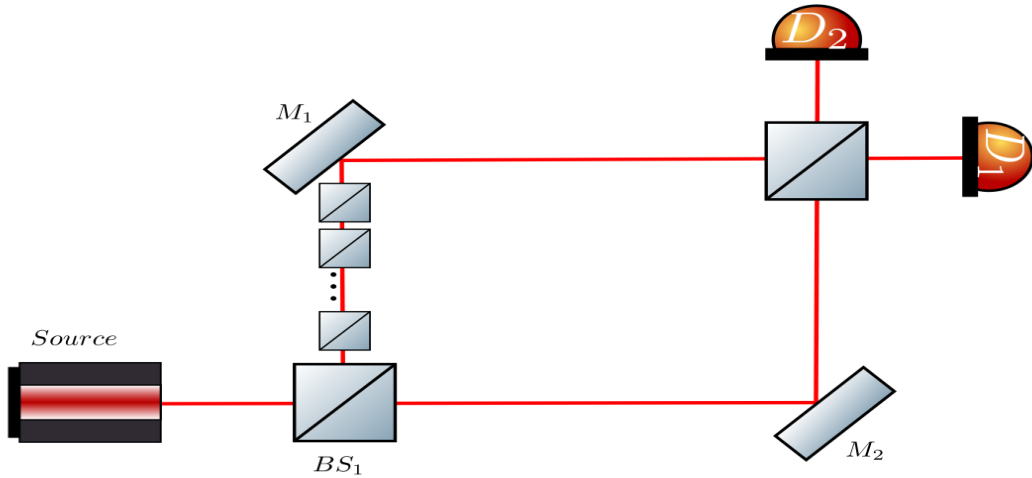
3.1 N Beam Splitters as imperfect absorber

Figure 7: Mach Zehnder with N BS as imperfect absorber

We begin analysing what happens if our initial state goes through several BS assuming the reflected photon is "lost". We will study both initial states in parallel,

as Fig.7 shows. We are placing N beams splitters in one of the paths of the interferometer so:

$$BS_1 \left|1\right\rangle = \cos(\theta_1) \left|1\right\rangle + i\sin(\theta_1) \left|abs\right\rangle. \tag{95}$$

$$BS_1 \left|2\right\rangle = \cos(\theta_1) \left|2\right\rangle + i\sin(\theta_1) \left|abs\right\rangle. \tag{96}$$

The next BS only acts on the transmitted photon so:

$$BS_2(\cos(\theta_1) \left|1\right\rangle + i\sin(\theta_1) \left|abs\right\rangle) = \cos(\theta_1)BS_2 \left|1\right\rangle + i\sin(\theta_1) \left|abs\right\rangle. \tag{97}$$

$$BS_2(\cos(\theta_1) \left|2\right\rangle + i\sin(\theta_1) \left|abs\right\rangle) = \cos(\theta_1)BS_2 \left|2\right\rangle + i\sin(\theta_1) \left|abs\right\rangle. \tag{98}$$

$$BS_2 BS_1 \left|2\right\rangle = \cos(\theta_1)\cos(\theta_2) \left|2\right\rangle + iA' \left|abs\right\rangle. \tag{99}$$

$$BS_2 BS_1 \left|1\right\rangle = \cos(\theta_1)\cos(\theta_2) \left|1\right\rangle + iA \left|abs\right\rangle. \tag{100}$$

Then, the next BS does the same

$$BS_3 BS_2 BS_1 \left|1\right\rangle = \cos(\theta_1)\cos(\theta_2)\cos(\theta_3) \left|1\right\rangle + iB \left|abs\right\rangle. \tag{101}$$

$$BS_3 BS_2 BS_1 \left|2\right\rangle = \cos(\theta_1)\cos(\theta_2)\cos(\theta_3) \left|2\right\rangle + iB' \left|abs\right\rangle. \tag{102}$$

so after n BS :

$$BS^n = BS_n...BS_3 BS_2 BS_1 \left|1\right\rangle = \cos(\theta_1)\cos(\theta_2)\cos(\theta_3)....\cos(\theta_n) \left|1\right\rangle + iC \left|abs\right\rangle. \tag{103}$$

$$BS^n = BS_n...BS_3 BS_2 BS_1 \left|2\right\rangle = \cos(\theta_1)\cos(\theta_2)\cos(\theta_3)....\cos(\theta_n) \left|2\right\rangle + iC' \left|abs\right\rangle. \tag{104}$$

We can obtain C and C' by asking the probabilities to add to unity, since everything that is not transmitted will be "lost":

$$BS^n \ket{1} = \prod_{i=1}^{n} \cos(\theta_i) \ket{1} + iD \ket{abs}. \tag{105}$$

$$BS^n \ket{2} = \prod_{i=1}^{n} \cos(\theta_i) \ket{2} + iD' \ket{abs}. \tag{106}$$

$$D' = D = \sqrt{1 - \prod_{i=1}^{n} \cos^2(\theta_i)} \tag{107}$$

We now use this as a imperfect absorber in the vertical path:

$$\ket{1} \xrightarrow{\text{BS1}} \cos(\theta_1) \ket{1} + i\sin(\theta_1) \ket{2}$$

$$\xrightarrow{B^n} \cos(\theta_1) \ket{1} + i\sin(\theta_1) \prod_{i=3}^{n} \cos(\theta_i) \ket{2} - \sin(\theta_1) \sqrt{1 - \prod_{i=3}^{n} \cos^2(\theta_i)} \ket{Abs}$$

$$\xrightarrow{\text{Mirrors}} \cos(\theta_1) e^{i\gamma_1} \ket{2} + i\sin(\theta_1) \prod_{i=3}^{n} \cos(\theta_i) e^{i\gamma_2} \ket{1} - \sin(\theta_1) \sqrt{1 - \prod_{i=3}^{n} \cos^2(\theta_i)} \ket{Abs}$$

$$\xrightarrow{\text{BS2}} \left(\cos(\theta_1)\cos(\theta_2) e^{i\gamma_1} - \sin(\theta_1)\sin(\theta_2) e^{i\gamma_2} \prod_{i=3}^{n} \cos(\theta_i) \right) \ket{2} +$$

$$i\left(\cos(\theta_1)\sin(\theta_2) e^{i\gamma_1} + \cos(\theta_2)\sin(\theta_1) e^{i\gamma_2} \prod_{i=3}^{n} \cos(\theta_i) \right) \ket{1} - \sin(\theta_1) \sqrt{1 - \prod_{i=3}^{n} \cos^2(\theta_i)} \ket{Abs}.$$

The probabilities of detection in each of the detectors are given by:

$$P_{D1} = |\cos(\theta_1)\sin(\theta_2)e^{i\gamma_1} + \cos(\theta_2)\sin(\theta_1)e^{i\gamma_2} \prod_{i=3}^{n} \cos(\theta_i)|^2. \tag{108}$$

$$P_{D2} = |\cos(\theta_1)\cos(\theta_2)e^{i\gamma_1} - \sin(\theta_1)\sin(\theta_2)e^{i\gamma_2} \prod_{i=3}^{n} \cos(\theta_i)|^2. \tag{109}$$

$$P_{Abs} = \sin^2(\theta_1)\left(1 - \prod_{i=3}^{n} \cos^2(\theta_i)\right). \tag{110}$$

3.2 Analysis with phase retarders

The interferometer is an instrument quite hard to align experimentally, in most cases alignment is a little off. We can characterize just how off this alignment is by considering the effects of phase retarders on the interferometer after all misalignment is nothing but differences in the optical path. Those predictions can be compared with the actual interferometer (without phase retarders), a wave retarder's matrix representation is:

$$Retarder = \begin{pmatrix} e^{ic} & 0 \\ 0 & e^{ik} \end{pmatrix} \tag{111}$$

.

Let's see the effect of such an optical device in our setup:

$$|1\rangle \xrightarrow{\text{BS1}} \cos(\theta_1)|1\rangle + i\sin(\theta_1)|2\rangle$$

$$\xrightarrow[\text{Absorber}]{\text{Imperfect}} cos(\theta_1)|1\rangle + i\sin(\theta_1)(\alpha'|abs\rangle + \beta'|2\rangle)$$

$$\xrightarrow[\text{Retarders}]{\text{Phase}} \cos(\theta_1)e^{ic}|1\rangle + i\beta'\sin(\theta_1)e^{ik}|2\rangle + i\alpha'\sin(\theta_1)|abs\rangle$$

$$\xrightarrow{\text{Mirrors}} \cos(\theta_1)e^{i(\gamma_1'+c)}|2\rangle + i\sin(\theta_1)\alpha'|abs\rangle + i\sin(\theta_1)\beta'e^{i(\gamma_2'+k)}|1\rangle,$$

we can stop here by noticing that making $\gamma_2' + k = \gamma_2$ and $\gamma_1' + c = \gamma_1$ we have the exact same case as in our previous sections, like in the section of a BS as an imperfect absorber with $\beta = cos(\theta_o)$ and $\alpha = i\sin(\theta_o)$ so our model that makes

use of the general matrix of a mirror instead of using the more popular perfect mirror matrix $M = \begin{pmatrix} i & 0 \\ 0 & i \end{pmatrix}$, where $i = e^{i\frac{\pi}{2}} = \gamma$, has the effect of a phase retarder included, allowing us to study misalignment.
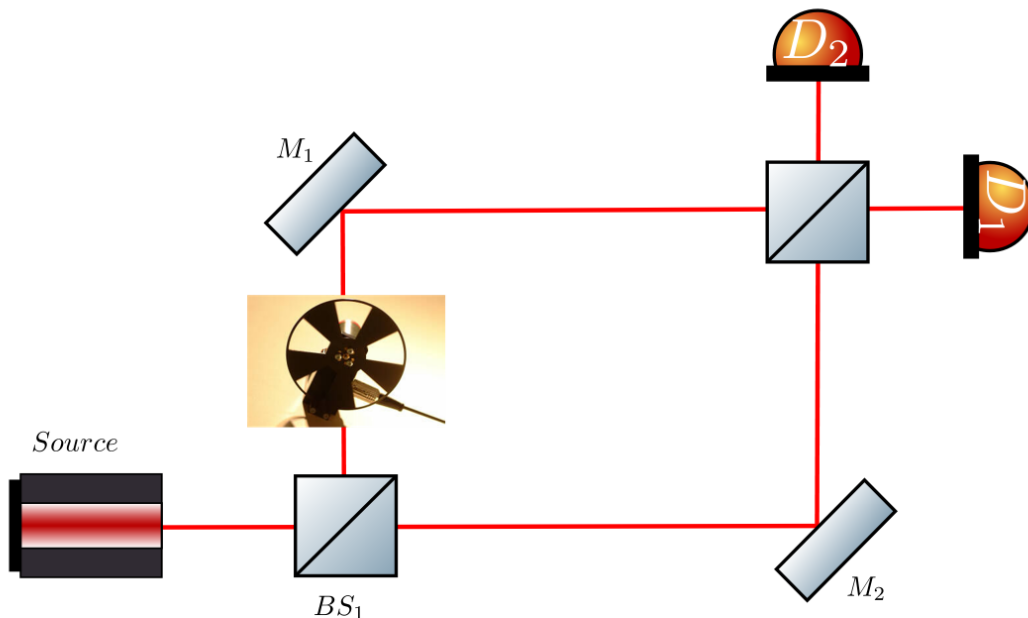
4 Optical chopper as perfect absorber

Figure 8: Mach-Zehnder with an optical chopper as an imperfect absorber

An optical chopper is a device that periodically interrupts light. It is usually a disk with holes rotating with a certain frequency (which can vary in time) from its definition we can infer that it can be modeled using a square wave which can be written as $f(t) = \frac{sgn(\sin(wt))+1}{2}$, where ω is the angular frequency of the optical chopper multiplied by the number of "hole-material" pairs which for now we assume are the same size.

We will be ignoring diffraction effects, a consequence of modeling it like this is that consecutive optical choppers become the product of square waves and products of square waves is again a square wave, so modeling many choppers would be the same as modeling one with that effective frequency, as Fig.8 shows. In this section we intend to analyze the Mach-Zenhder interferometer with a chopper being the

imperfect absorber, the chopper introduces a discrete time dependence, therefore we will be alternating between two different probability distributions.

We can model our optical chopper by using an operator C_i where i is the path where the chopper is placed, such that in our base(where $i = 1, 2$ and $i \neq j$):

$$C_i \left| i \right\rangle = f(t) \left| i \right\rangle . \tag{112}$$

$$C_j \left| i \right\rangle = \left| i \right\rangle . \tag{113}$$

Ideally we want this operator to be unitary in the "hole" cycle. Since we are modeling the whole as a totally transparent object. This will be checked right away:

$$|f|^2 = \frac{(sgn(\sin(wt) + 1)^2}{4}, \tag{114}$$

the sign function squared is always one so

$$|f|^2 = \frac{2(1 + sgn(\sin(wt)))}{4}. \tag{115}$$

$$|f|^2 = f, \tag{116}$$

from there we can see that it is a unitary matrix whenever the sine is in the positive cycle, and it becomes null in the negative cycle, that happens because in the negative cycle we have total absorption. The absorption coefficient would be:

$$a = 1 - f. \tag{117}$$

$$a = \frac{1 - sgn(\sin(wt))}{2}. \tag{118}$$

$$|a|^2 = \frac{2(1 - sgn(\sin(wt)))}{4}. \tag{119}$$

$$|a|^2 = a. \tag{120}$$

We will now analyze a Mach-Zehnder interferometer using a chopper as an time dependent absorber. The chopper will be placed on the vertical path, and our photon will go into the interferometer using the horizontal path

$$|1\rangle \xrightarrow{\text{BS1}} \cos(\theta_1)|1\rangle + i\sin(\theta_1)|2\rangle$$

$$\xrightarrow{\text{Chopper}} \cos(\theta_1)|1\rangle + i\sin(\theta_1)f|2\rangle + i\sin(\theta_1)a|abs\rangle$$

$$\xrightarrow{\text{Mirrors}} \cos(\theta_1)e^{i\gamma_1}|2\rangle + i\sin(\theta_1)fe^{i\gamma_2}|1\rangle + i\sin(\theta_1)a|abs\rangle$$

$$\xrightarrow{\text{BS2}} \cos(\theta_1)e^{i\gamma_1}(\cos(\theta_2)|2\rangle + i\sin(\theta_2)|1\rangle) + i\sin(\theta_1)e^{i\gamma_2}f(\cos(\theta_2)|1\rangle + i\sin(\theta_2)|2\rangle) + i\sin(\theta_1)a|abs\rangle$$

$$= i(e^{i\gamma_1}\cos(\theta_1)\sin(\theta_2) + fe^{i\gamma_2}\sin(\theta_1)\cos(\theta_2))|1\rangle + (\cos(\theta_1)\cos(\theta_2)e^{i\gamma_1} -$$

$$\sin(\theta_1)\sin(\theta_2)fe^{i\gamma_2})|2\rangle + i\sin(\theta_1)a|abs\rangle. \tag{121}$$

A plot for the detection probabilities is shown in Fig.9, as we mentioned before the system is alternating between two probability distributions. We can see those for each of the possible states in the figure. It is worth noting that the absorption graph alternates between the one shown and no absorption:

$$P_{2D1} = |e^{i\gamma_1}\cos(\theta_1)\sin(\theta_2) + fe^{i\gamma_2}\sin(\theta_1)\cos(\theta_2)|^2. \tag{122}$$

$$P_{2D2} = |\cos(\theta_1)\cos(\theta_2)e^{i\gamma_1} - f\sin(\theta_1)\sin(\theta_2)e^{i\gamma_2}|^2. \tag{123}$$

$$P_{2Abs} = |a\sin(\theta_1)|^2. \tag{124}$$

Which can be rewritten as:

$$P_{2D1} = \cos^2(\theta_1)\sin^2(\theta_2) + f^2\sin^2(\theta_1)\cos^2(\theta_2) + \frac{f\sin(2\theta_1)\sin(2\theta_2)\cos(\gamma_1 - \gamma_2)}{2}. \tag{125}$$

$$P_{2D2} = \cos^2(\theta_1)\cos^2(\theta_2) + f^2\sin^2(\theta_1)\sin^2(\theta_2) - \frac{f\sin(2\theta_1)\sin(2\theta_2)\cos(\gamma_1 - \gamma_2)}{2}. \tag{126}$$

$$P_{2Abs} = a^2\sin^2(\theta_1). \tag{127}$$

(a) P_{1Abs}

(b) P_{2D2} in the first cycle

(c) P_{2D2} in the second cycle

(d) P_{2D1} in the first cycle
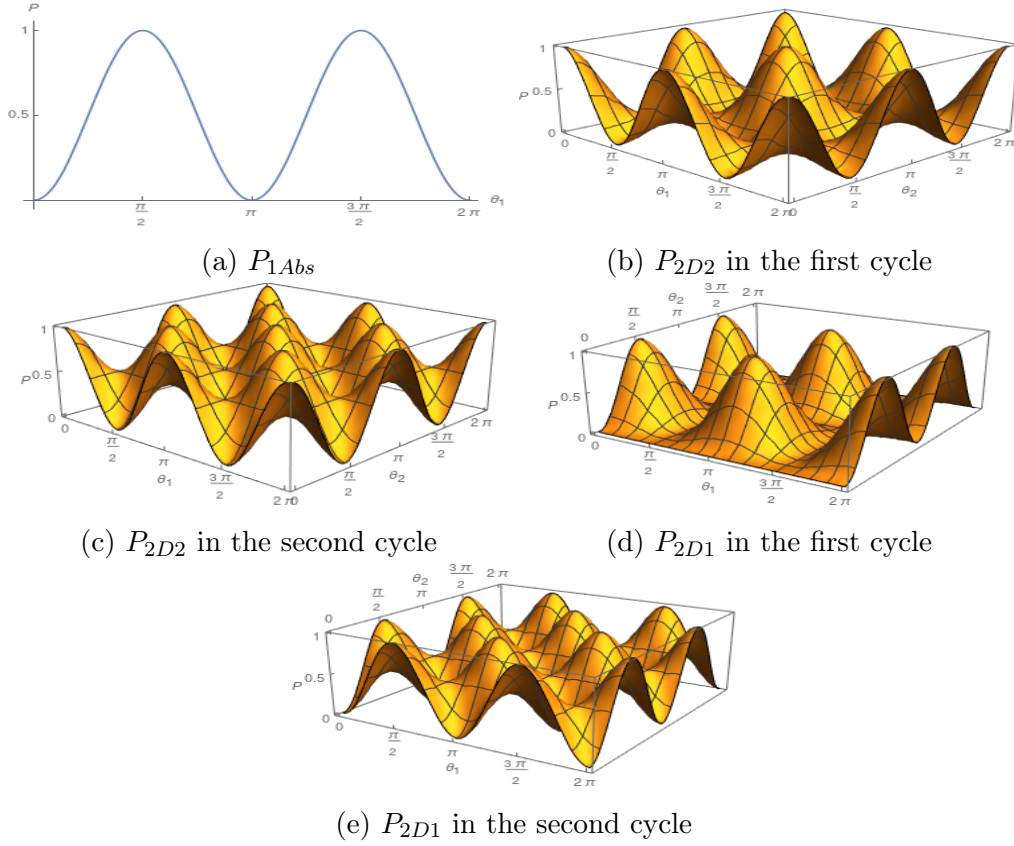

(e) P_{2D1} in the second cycle

Figure 9: Probability Distribution for $\gamma_2 - \gamma_1 = \frac{\pi}{2}$ in the vertical path

By the exact same procedure having the chopper in the horizontal path, one can obtain the following results which are shown in Fig.9, for each of the possible states of the system

$$P_{1D1} = \cos^2(\theta_1)\sin^2(\theta_2)f^2 + \sin^2(\theta_1)\cos^2(\theta_2) + \frac{f\sin(2\theta_1)\sin(2\theta_2)\cos(\gamma_1 - \gamma_2)}{2}.$$

(128)

$$P_{1D2} = \cos^2(\theta_1)\cos^2(\theta_2)f^2 + \sin^2(\theta_1)\sin^2(\theta_2) - \frac{f\sin(2\theta_1)\sin(2\theta_2)\cos(\gamma_1 - \gamma_2)}{2}.$$

(129)

$$P_{2Abs} = a^2\cos^2(\theta_1).$$

(130)

(a) P_{1Abs}

(b) P_{1D2} in the first cycle

(c) P_{1D2} in the second cycle

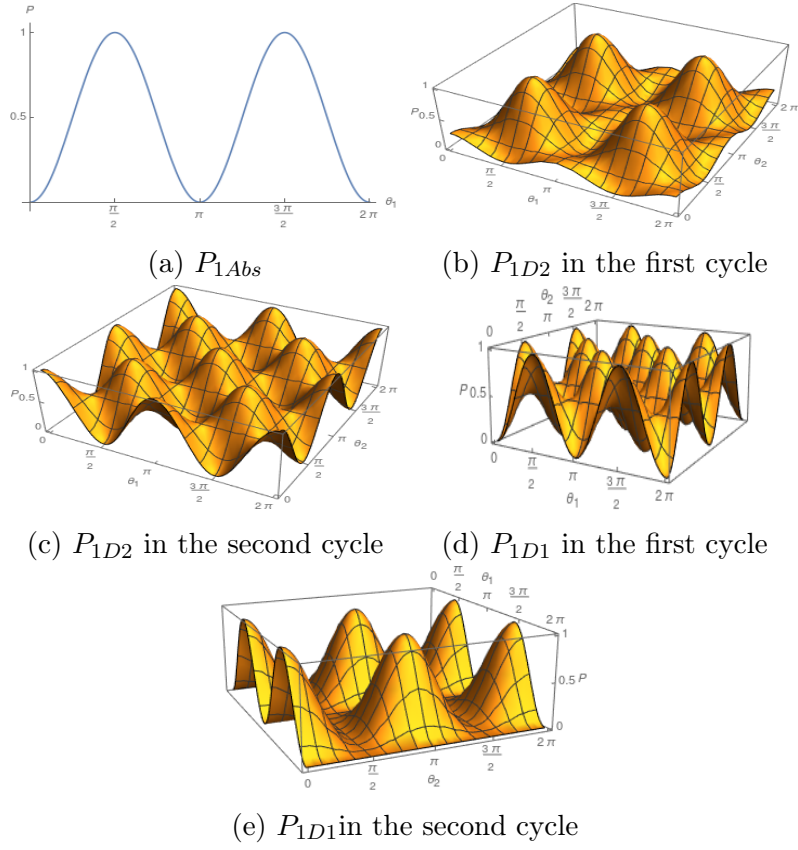(d) P_{1D1} in the first cycle

(e) P_{1D1} in the second cycle

Figure 10: Probability distribution for the horizontal path and $\gamma_2 - \gamma_1 = \frac{\pi}{2}$

Since $f^2 = f$, we can write the difference of probabilities as:

$$P_{1D1} - P_{1D2} = (a) \left(\frac{\cos(2\theta_1) - \cos(2\theta_2)}{2} \right). \tag{131}$$

$$P_{2D1} - P_{2D2} = (a) \left(\frac{\cos(2\theta_1) + \cos(2\theta_2)}{2} \right). \tag{132}$$

From there we can obtain either θ_1 or θ_2 :

$$(P_{1D1} - P_{1D2}) + (P_{2D1} - P_{2D2}) = (a)(\cos(2\theta_1)). \tag{133}$$

$$(P_{1D1} - P_{1D2}) - (P_{2D1} - P_{2D2}) = (-a)(\cos(2\theta_2)). \tag{134}$$

$$\theta_1 = \frac{1}{2} \cos^{-1} \left[\frac{(P_{1D1} - P_{1D2}) + (P_{2D1} - P_{2D2})}{a} \right]. \tag{135}$$

$$\theta_2 = \frac{1}{2} \cos^{-1} \left[\frac{(P_{1D1} - P_{1D2}) - (P_{2D1} - P_{2D2})}{a} \right]. \tag{136}$$

4.1 Optical chopper as imperfect absorber

Previously we considered the "material" part of the chopper as a perfect absorber. In this section we will now generalize to when it is an imperfect absorber, this can be done quite simply by defining :

$$f_{hole} = \frac{1 + sgn(\sin(wt))}{2}. \tag{137}$$

$$f_{material} = \left(\frac{1 - sgn(\sin(wt))}{2} \right) \beta. \tag{138}$$

$$f = f_{material} + f_{hole}. \tag{139}$$

Where β is the transmission coefficient of the material part of our chopper, β could be a function of ω or t in this analysis. The operator used to describe our chopper is the same as in the previous section, we define:

$$a = \left(\frac{1 - sgn(\sin(wt))}{2} \right) \alpha. \tag{140}$$

Where α is the absorption coefficient of the material part of our chopper, by using this notation we have the exact same case as in the previous section, except this time $f^2 \neq 1$:

$$|a|^2 = a\alpha. \tag{141}$$

$$|f_{material}|^2 = f_{material}\beta, \tag{142}$$

which we can generalize to obtain:

$$|a|^n = a\alpha^{n-1}. \tag{143}$$

$$|f_{material}|^n = f_{material}\beta^{n-1}, \tag{144}$$

so we have:

$$|f|^2 = \frac{|\alpha|^2}{2} sgn(\sin(wt)) + \frac{1 + |\beta|^2}{2}. \tag{145}$$

Substituting in the previous section yields the probability distributions shown in Fig.11:

(a) P_{1Abs}

(b) P_{1D2} in the first cycle

(c) P_{1D2} in the second cycle

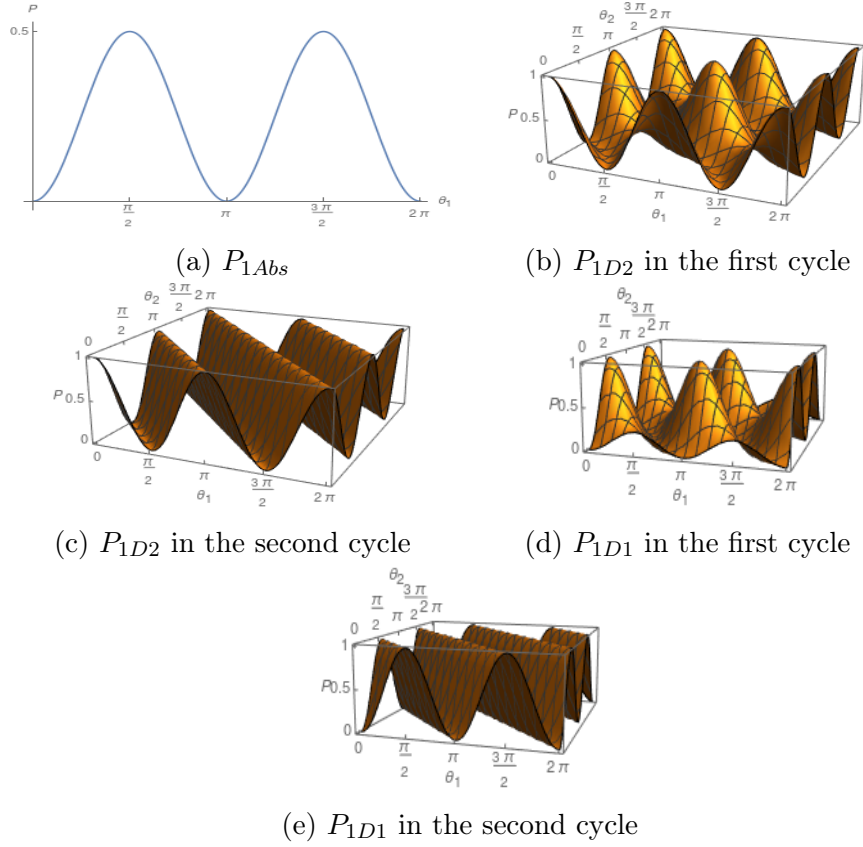(d) P_{1D1} in the first cycle

(e) P_{1D1} in the second cycle

Figure 11: Probability Distribution in the horizontal path with $\gamma_2 - \gamma_1 = 0$ y $\beta = 0.5$

$$P_{1D1} = \cos^2(\theta_1)\sin^2(\theta_2)|f|^2 + \sin^2(\theta_1)\cos^2(\theta_2) + \frac{\text{Re}\{f\}\sin(2\theta_1)\sin(2\theta_2)\cos(\gamma_1 - \gamma_2)}{2}.$$

$$(146)$$

$$P_{1D2} = \cos^2(\theta_1)\cos^2(\theta_2)|f|^2 + \sin^2(\theta_1)\sin^2(\theta_2) - \frac{\text{Re}\{f\}\sin(2\theta_1)\sin(2\theta_2)\cos(\gamma_1 - \gamma_2)}{2}.$$

$$(147)$$

$$P_{1Abs} = |\alpha|^2\cos^2(\theta_1).$$

$$(148)$$

When the optical chopper is in the vertical path we obtain the following detection probabilities. The probability distributions are shown in Fig.12:

(a) P_{1Abs}

(b) P_{2D1} in the first cycle

(c) P_{2D1} in the second cycle

(d) P_{2D1} in the first cycle
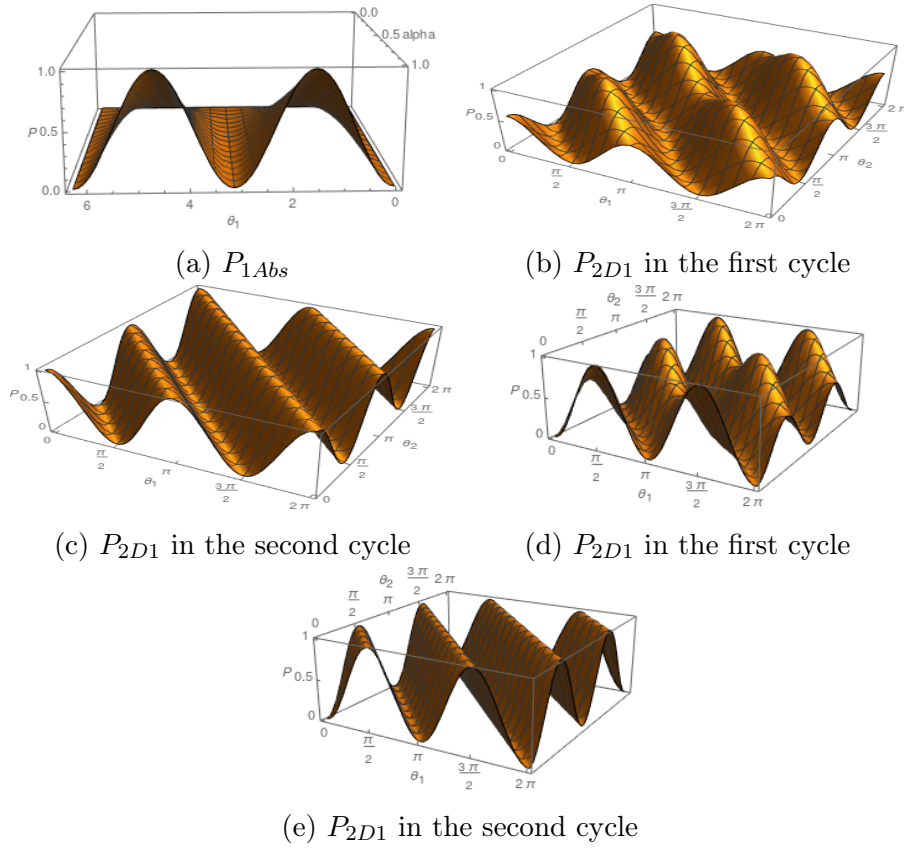
(e) P_{2D1} in the second cycle

Figure 12: Probability Distribution for the vertical path with $\gamma_2 - \gamma_1 = 0$ y $\beta = 0.5$

$$P_{2D1} = \cos^2(\theta_1) \sin^2(\theta_2) + |f|^2 \sin^2(\theta_1) \cos^2(\theta_2) + \frac{\text{Re}\{f\} \sin(2\theta_1) \sin(2\theta_2) \cos(\gamma_1 - \gamma_2)}{2}.$$

(149)

$$P_{2D2} = \cos^2(\theta_1) \cos^2(\theta_2) + |f|^2 \sin^2(\theta_1) \sin^2(\theta_2) - \frac{\text{Re}\{f\} \sin(2\theta_1) \sin(2\theta_2) \cos(\gamma_1 - \gamma_2)}{2}.$$

(150)

$$P_{2Abs} = |\alpha|^2 \sin^2(\theta_1).$$

(151)

5 Analysis of N intereferometers

The notation previously used is not popular when dealing with nested interferometers. In order to be consistent with the existing literature we will use the same notation as Kwait et al.[17], where we have an interferometer like the one in the following Fig.13, we see from the figure that we will have N BS and $N-1$ Absorbers:
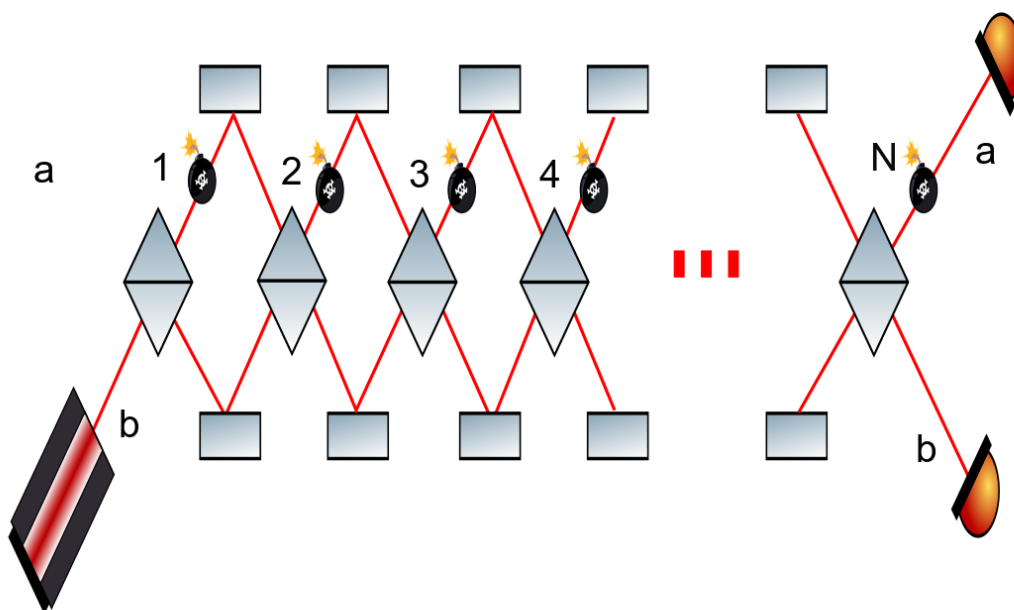

Figure 13: Nested Mach-Zehnders with imperfect absorbers

We will still use a binary basis, but instead of using the Horizontal-Vertical, it will be a path A-path B basis. That is a "up-down" basis, we will use $|2\rangle$ for path b and $|1\rangle$ for path a, one of the main advantages of this basis is that the mirror matrices are diagonal, because they keep our photon on the same path. We will model our imperfect absorber using a non-unitary diagonal matrix just as was done by Azuma [16].

Azuma used a matrix of the form, where $n = |\beta|^2$:

$$A_{Azuma} = \begin{pmatrix} \sqrt{n} & 0 \\ 0 & 1 \end{pmatrix}. \tag{152}$$

Since we are using a BS as an imperfect absorber a more suitable option would be
:

$$A_{BS} = \begin{pmatrix} \cos(\theta) & 0 \\ 0 & 1 \end{pmatrix}. \tag{153}$$

The final state can be obtained by applying all of the operators to the initial state which will be $|2\rangle$, Let us first consider that we have no imperfect absorbers on the interferometer, then the only operators acting on the state are BS then:

$$BS_i \times BS_{i+1} = \begin{pmatrix} \cos(\theta_i) & i\sin(\theta_i) \\ i\sin(\theta_i) & \cos(\theta_i) \end{pmatrix} \begin{pmatrix} \cos(\theta_{i+1}) & i\sin(\theta_{i+1}) \\ i\sin(\theta_{i+1}) & \cos(\theta_{i+1}) \end{pmatrix}. \tag{154}$$

$$= \begin{pmatrix} \cos(\theta_i)\cos(\theta_{i+1}) - \sin(\theta_i)\sin(\theta_{i+1}) & i(\cos(\theta_{i+1})\sin(\theta_i) + \cos(\theta_i)\sin(\theta_{i+1})) \\ i(\cos(\theta_{i+1})\sin(\theta_i) + \cos(\theta_i)\sin(\theta_{i+1})) & \cos(\theta_i)\cos(\theta_{i+1}) - \sin(\theta_i)\sin(\theta_{i+1}) \end{pmatrix}. \tag{155}$$

$$= \begin{pmatrix} \cos(\theta_i + \theta_{i+1}) & i\sin(\theta_i + \theta_{i+1}) \\ i\sin(\theta_i + \theta_{i+1}) & \cos(\theta_i + \theta_{i+1}) \end{pmatrix}, \tag{156}$$

if we assume N BS that are identical:

$$BS^N = \begin{pmatrix} \cos(N\theta) & i\sin(N\theta) \\ i\sin(N\theta) & \cos(N\theta) \end{pmatrix} \tag{157}$$

Let's assume $\theta = \frac{\pi}{2N}$ so we have:

$$BS^N = \begin{pmatrix} 0 & i \\ i & 0 \end{pmatrix}, \tag{158}$$

so we will always detect the photon in the path that is not the the one we sent

our photon in, with this in mind let us see what happens with this particular θ when we do have imperfect absorbers. The state first goes through a BS, then one of the imperfect absorbers and then another BS, it keeps going like that until it encounters the Nth and last BS. We have N BS and $N-1$ imperfect absorbers so our final state is:

$$|2\rangle \xrightarrow[\text{interferometers}]{\text{Nested}} (B \times A)^{N-1} B |2\rangle . \tag{159}$$

Detection probabilities are given by:

$$P_{D1} = |\langle 2| (B \times A)^{N-1} B |2\rangle|^2. \tag{160}$$

$$P_{D2} = |\langle 1| (B \times A)^{N-1} B |2\rangle|^2. \tag{161}$$

$$P_{Abs} = 1 - P_{D1} - P_{D2}. \tag{162}$$

To obtain said probabilities as well as the behaviour of the system for varying N we will make use of a computer. The program was written in python and yielded the following results:

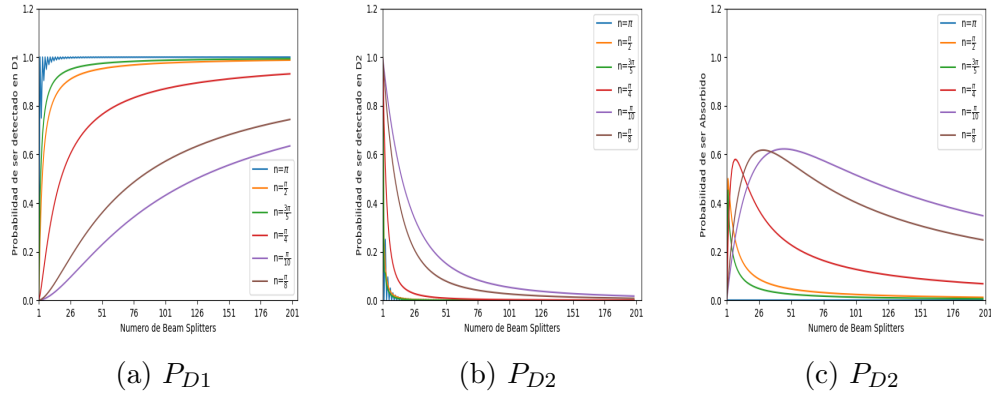(a) P_{D1} (b) P_{D2} (c) P_{D2}

Figure 14: Probabilities when BS is an imperfect absorber, D1 is in path b, and D2 in path a

Fig.14 shows the different probabilities for absorption, and detection as we increase

N. We can see this asymptotically approaches 1 as Azuma had shown [16], the case of a BS as an absorber shows consistency. This is important because the case of a BS is described by the same mathematics that and analyzer and a polarizer [?] and unlike other absorbers this can be manipulated continually, giving us a way to test this curves experimentally.

One may wonder how the system behaves for growing N with the same kind of BS for all N, maybe we could make the probabilities grow as well, but after the analysis. We can see that even though it grows for low N it soon begins to lower and approaches 0 very quickly for most values as we can see below.
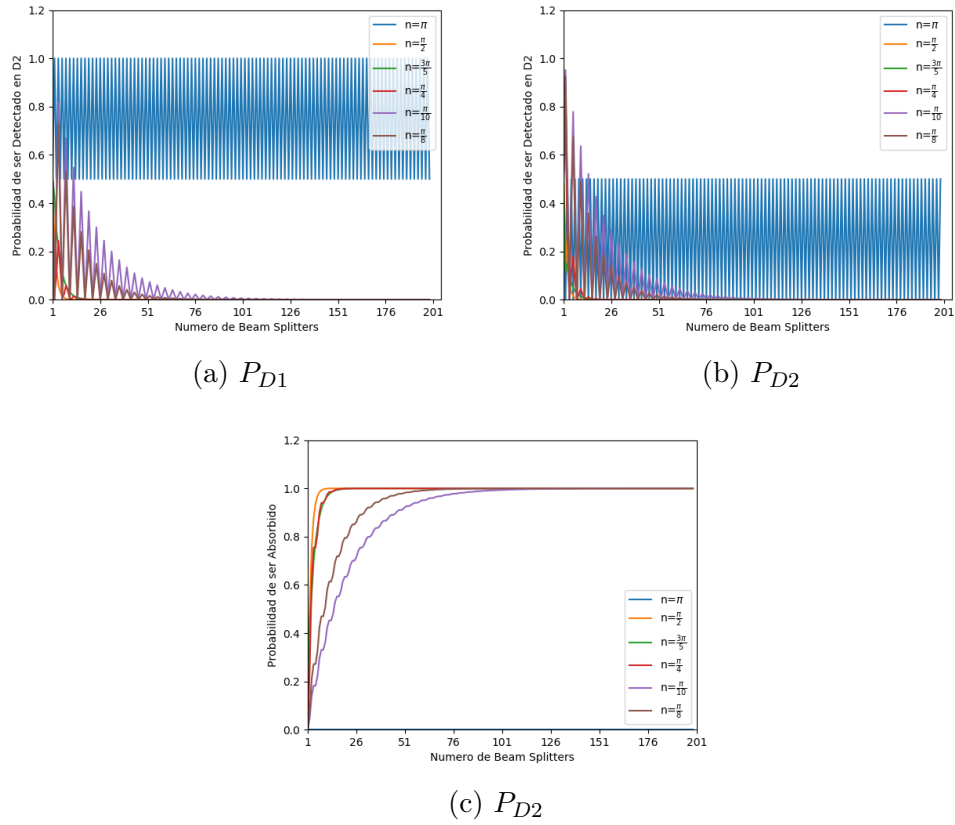

(a) P_{D1}

(b) P_{D2}

(c) P_{D2}

Figure 15: Behavior for growing N 50/50 BS for all N

Fig.15 shows the probabilities when we increase the number of interferometers but do not change the value of the BS as N increases, this may seem like a waste of effort since the aim is to maximize the detection probability. However let us

assume that the we actually have an absorber that has a very little absorption probability, if we wanted to have it absorbing our photon this scheme would prove useful

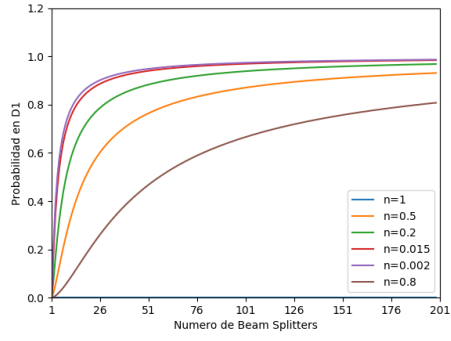## 5.1 Optical chopper as imperfect absorber in N interferometers

For an optical chopper the following matrix could be used:

$$A_{chopper} = \begin{pmatrix} f & 0 \\ 0 & 1 \end{pmatrix}.$$ (163)

However as f only varies discretely our matrix will alternate between two values of n,between two transparencies :

$$f = \left(\frac{1 - sgn(\sin(wt))}{2} \right) \beta + \frac{1 + sgn(\sin(wt))}{2}.$$ (164)

in the positive cycle we have $f_{positive} = 1$. While on the negative cycle $f_{negative} = \beta$. For convenience we will redefine $n = |\beta|^2$ and write in terms of n, this way in the positive cycle we will have the case of the nested interferometer with no object which is the same as $\beta = 1$, but in the negative cycle we will have Azuma's case. We now use Azuma's matrix to perform the same analysis and also realize the probabilities will alternate between the blue line $\beta = 1$ and and the line which is $\beta = Transmittance$ of our chopper:

(a) P_{D1}
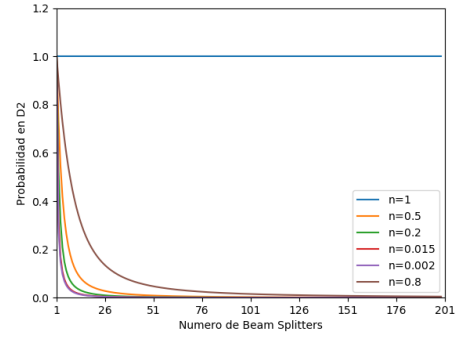
(b) P_{D2}
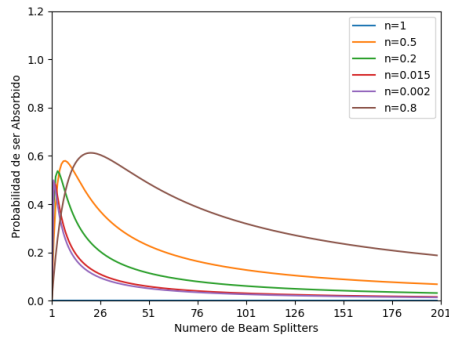
(c) P_{D2}

Figure 16: Behavior for Growing N for a chopper as imperfect absorbers

Fig.16 shows the probabilities of a given absorber, the blue line represents the "hole" part of the chopper, and the other lines represent the "material" part, the system will alternate periodically between these probabilities

6 Experimental Setup

In this section we will describe the necessary materials and steps to realize all of the previous content of this thesis experimentally. All of the work from this section on took place at the laboratory for quantum and electromagnetic phenomena at UPIITA. We will begin by generating a single photon source using SPDC, we will follow the approach taken in [18]. We will then replicate the Elitzur-Vaidman "bomb detector". Finally we will study variations of this "bomb detector" with semitransparent objects.

6.1 Single photon source

In order to produce single photons we will use the SPDC process described in section 1, to do this experimentally we will follow the method described in [18]. The experimental setup can be seen in the Fig.17. We will use the following materials:

- Aluminum rails

- Infrared filters 810nm $\pm$ 10nm

- Violet laser 405nm

- Pinholes

- BBO-I crystal

- Multimode optical fiber

- APDs(Avalanche photo-diodes)

- National instruments' data acquisition board

- Piezoelectric Thorlabs AE0505D-16F
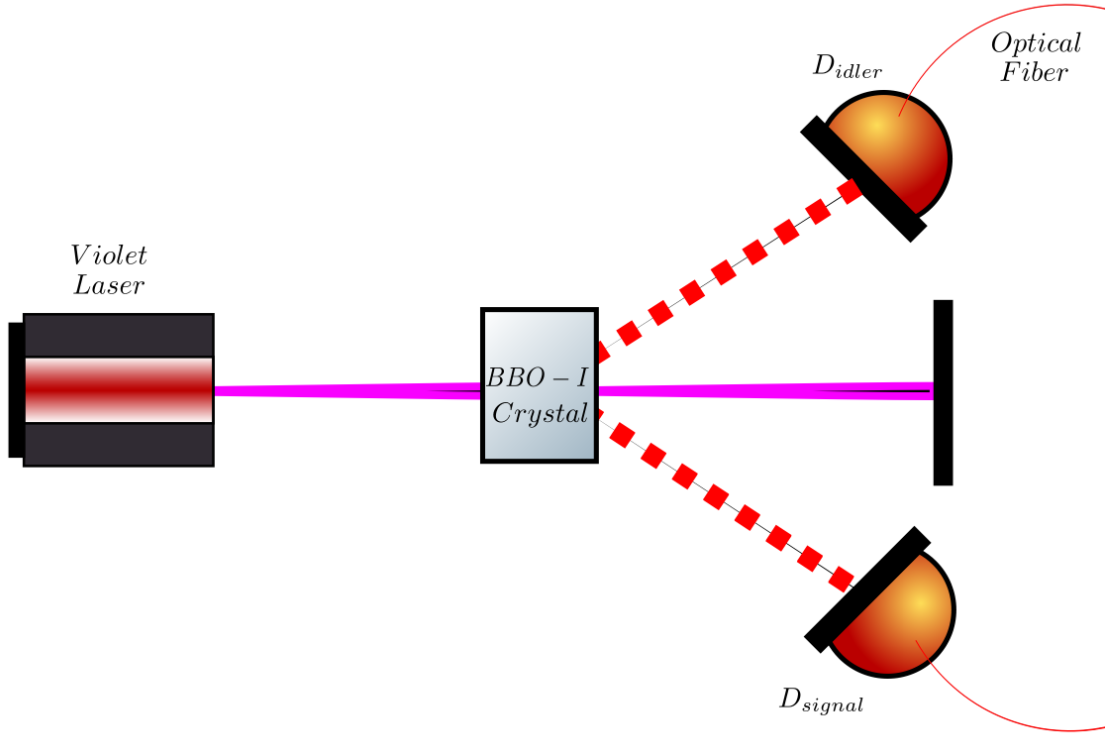
- Newport posts

- Optical Table

Figure 17: Experimental setup of single photon source

The first step to achieve the single photon source is to find the most likely light-cone using individual counts in each photo-detector, after that we need to count coincidences to identify spatial correlations. We will set the detection window for coincidences at 10ns, this coincidence window is used so we know the pair of photons is actually created in the nonlinear crystal thus eliminating noise from the environment in the detection counts. It is usually convenient for the propagation direction of the photon to be co-lineal with one of the lines of tapped holes

In BBO-I crystals both photons have the same energy, from Eq.1 we can see that this implies that both signal and idler photons' direction of propagation make the same angle with respect to the pump's as seen in Fig.17.

Since we know the relationship between each of the propagation directions, and it is in our best interest to have the signal photon co-lineal to the tapped holes, we will make the necessary adjustments so this happens. This is usually done by first

setting the laser pump to be co-linear to the tapped holes, and then rotating both the laser and the crystal in such a way that the laser propagates in the direction previously occupied by the idler photon while the signal photon propagates in the direction previously occupied by the laser. The new direction of the idler photon can be found using Eq.1

Once we achieve this, we place APDs in the direction of propagation of both signal and idler photons. Our single photon source is ready to go and the next step we need to take is to set up and align the Mach-Zehnder interferometer.

6.2   Single photon Mach-Zehnder interferometer

As we previously described in section 1 the Mach-Zehnder interferometer is made of two Beam splitters (BS_1 and BS_2) and two mirrors(M_1 and M_2), to realize this device experimentally we will need those. As the Eliztur-Vaidman "bomb detector" uses $50 : 50$ beam splitters we will set up our interferometer using those. In adition to the previous section we will need:

- Two 50:50 Beam splitters

- Two mirrors

- Red laser 700nm

- Incandescent white light source

We aim to get the difference in optical paths to a minimum, that is as we explored in section 2.4.3, we wish to achieve $|\gamma_2 - \gamma_1| = 0 + 2\pi n$, this alignment can be quite challenging in the laboratory. In order to achieve this we will consider the following approach for alignment as discussed in [14]. To align the interferometer and reduce $|\gamma_2 - \gamma_1|$ as much as possible, the strategy is to attach a piezoelectric device to one of the mirrors, align it by hand and then varying the voltage applied to the piezoelectric (changing this mirror's orientation) until a minimum is reached.

Both D_1 and D_2 are APDs placed in the same way as in Fig.1, in the output of BS_2, the interference pattern requires special treatment of the counts, since

unlike the classical case where we inject coherent beams into the interferometer we are injecting single photons. This "special treatment" consists in only considering detector clicks when there's a simultaneous coincidence in D_{idler}, where D_{idler} is an APD placed in the path of the idler photon as described in the SPDC section, we will use the same temporal window of "simultaneously" as described in section 6.1 that is 10ns. The experimental set up for this section is shown in Fig.18
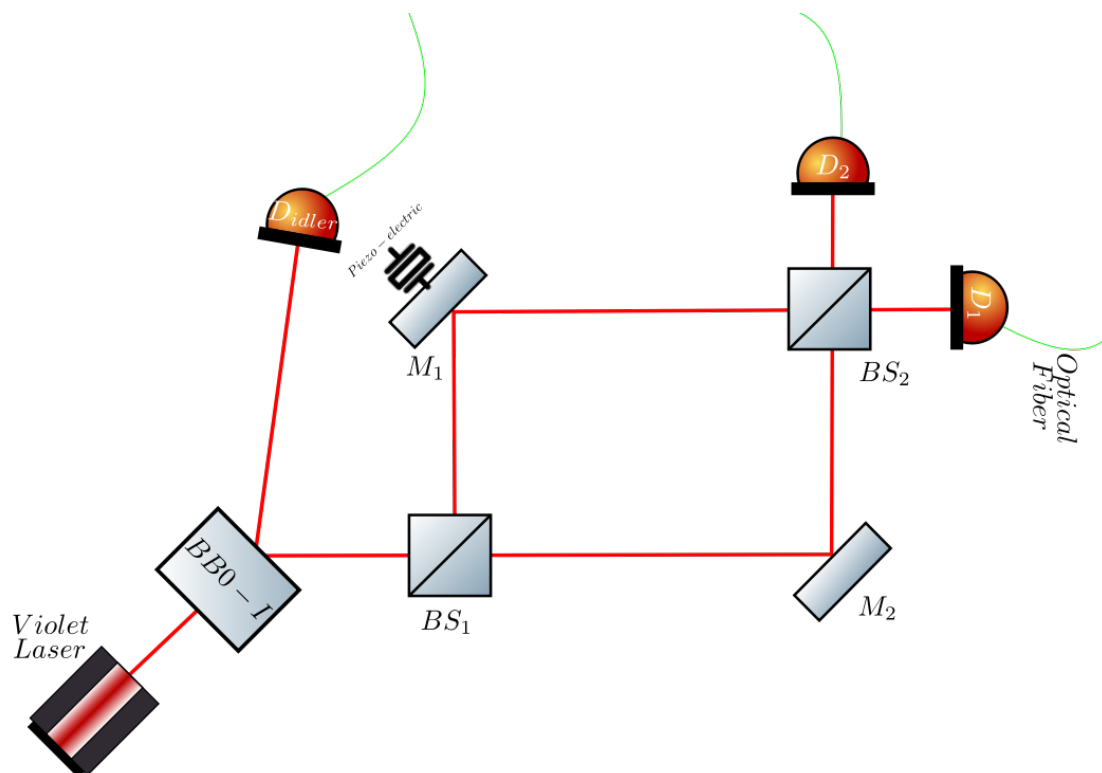

Figure 18: Experimental setup of a single photon Mach-Zehnder Interferometer

6.2.1 Alignment of the Interferometer

In this section we will describe in detail the procedure used to align the Mach-Zehnder interferometer this approach was used in [14], as mentioned before the idea is to get $|\gamma_2 - \gamma_1| = 2\pi n$. To do this it is necessary to be rigorous regarding the optical devices' position and characteristics, for instance it is necessary to consider that the BS faces are not completely flat, this is a problem because a BS

can change the propagation direction of the transmitted beam even when placed at $\theta = 45°$. We will use $BS_1 = BS_2 = 50 : 50$

To align the interferometer we begin by placing a red laser(HeNe) in such a way that the beam goes through the same path as the signal photon. To do this two collimators are needed. One is placed as closed as possible to the BBO-I crystal, and the other one is placed near the D_{signal} from the SPDC array. All alignment of our Mach-Zehnder is done using this red laser.

The first step is to place BS_1 at $\theta = 45°$ with respect to the incoming beam. Additionally, both the transmitted and reflected beam must be co-lineal to the tapped holes in the optical table. Using two "screens" we will mark where both the transmitted and reflected photons go as shown in Fig.19 (a-d) show all the steps we are going to take to align.

The second step is to place one of the mirrors M_2 in the path of the transmitted beam, the idea is to place M_2 in such a way that the reflected beam is co-lineal with the tapped holes of the optical table, and then mark on the screen the place where the beam goes, as is shown in Fig.19(b). .

The third step is to dismount M_2(Only the mirror it isn't necessary to take out the ¿post?(no se si se diga asi)) and to place M_1 and repeat step to using M_1 instead of M_2. We will place one of the mirrors in a ¿post? with a micro-metric screw and piezoelectric device to obtain vertical mobility, We will choose M_1, after completing this step we place M_2 once again, the expected result so far is shown in Fig.19(c)

The fourth and last step is to place BS_2 as it is shown in Fig.19(d), the reflected and transmitted beam should reach the marks done in step three, since we are working with a coherent beam we will see the interference pattern achieved on the screen. Once we've achieved the desired interference pattern, this same setup should be tested with white light from an incandescent source, that is because the coherence-length of the red laser is very long, so it is relatively easy to get red interference. After we have tested with white light we will place the APDs on those marks.
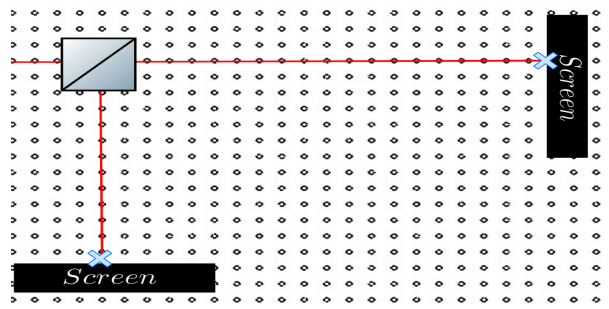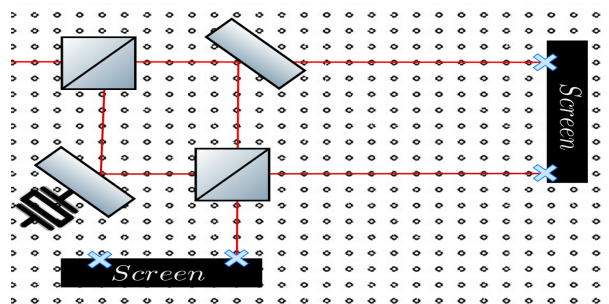
(a) First step
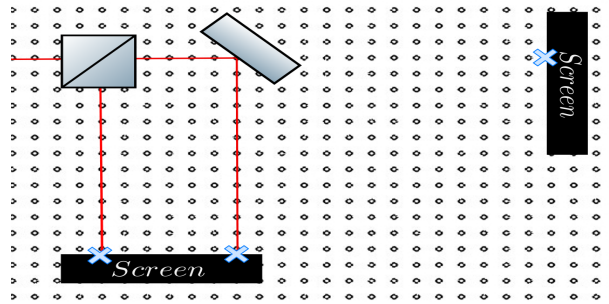
(b) Second step
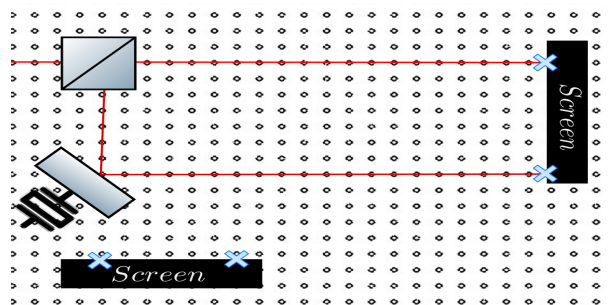
(c) Third step

(d) Fourth and last step

Figure 19: Steps to align the Mach-Zehnder interferometer

We make the Mach-Zehnder interferometer as small as possible, this allows a better control over the length of the optical paths making alignment easier.

6.2.2 Single photon interference

Once we've aligned the interferometer we can use our single photon source as input, that is we replace the red laser for the single photon source. We will count count coincidences between $D_{idler} - D_1$ and $D_{idler} - D_2$ in a temporal window of 10ns. The count pairs over the total counts will give us the probabilities.

Once we've done all of this we are ready to start the experiments that mainly concern this thesis, we will begin by replicating the "Elitzur-Vaidman" experiment, and then move on to the variations with semitransparent objetcs

• Perfect absorber

In order to have an imperfect absorber we will use a polarizer and an analyzer, since we are using type-I SPDC (we are using a BBO-I crystal) we know that both the signal and idler photon will have identical polarizations and that it will be orthogonal to that of the photon. We can fabricate a perfect absorber by rotating the analyzer. This is because as Malus' law states [19]

$$I = I_0 \cos^2(\theta) \tag{165}$$

where I_0 is the intensity before the polarizer and analyzer, I is the intensity after them, and θ is the angle between the polarizer and analyzer, if we rotate them in such a way that $\theta = 0$ then we have our perfect absorber that can be placed in one of the arms of our interferometer

The Quantum version of this law is very similar [20] a generalization for fermions was also obtained. Therefore this analogy is valid both in the classical and quantum regime.

• Semitransparent Objects

The behavior of a BS is analogous to that of an analyzer and polarizer(same transmission and reflection/absorption coefficients) as Leonhartd states in [21] a pictorial diagram of the analogy is shown in Fig.20, so in order to get a fair number of experimental points in the BS as imperfect transmitter curves, we will use a polarizer and analyzer and vary θ, the "lost" photon will be absorbed instead. The same idea will be used for the N beam-splitter section. Curves will be made once we know with how many we can count in the laboratory, that way setting N.
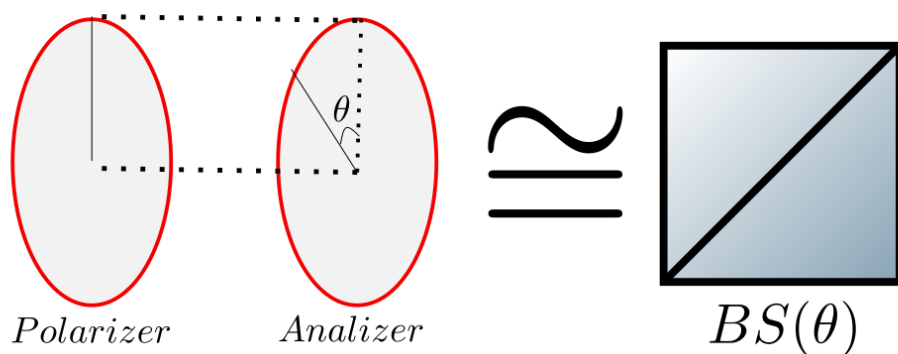

Figure 20: Diagram of the analogy between a polarizer and an analizer and a BS

An interesting experiment that could be replicated and generalized if time allows is the realization of "N interferometers" as Kwait et al. realized in [22], where taking advantage of this analogy and exploiting the quantum Zeno effect [23] designed a version of this experiment that requires just a few optical devices, a semitransparent object could be placed in this setup enabling us to compare with the curves in section 5.

In the case of the chopper, one with perfect absorption would be quite difficult to implement, therefore this curves may not be tested and remain pending work, in the case of the chopper as an imperfect absorber the idea is to 3d print an optical chopper that is hollow and can be field with different powders and liquids, changing its optical properties, the downside of this approach is that every time we fill it with something different it's optical properties must be characterized.(DISCUTIR ESTO CON ASESORES).

6.2.3 Varying optical paths

In order to be able to see the interference pattern, it is necessary to adjust the difference in optical paths $\delta\phi$. Visibility is a quantitative measure of the quality of the interference pattern, classically it is defined as [19]:

$$V = \frac{I_{max} - I_{min}}{I_{max} + I_{min}}, \tag{166}$$

where I_{max} is the maximum intensity and I_{min} is the minimum intensity of the interference pattern. The ideal pattern has perfect visibilty(V=1), which happens when $I_{min} = 0$.

In quantum mechanics the intensity is proportional to the expected value of the photon number [24], so the visibility is then given by:

$$V = \frac{N_{max} - N_{min}}{N_{max} + N_{min}}, \tag{167}$$

In the lab N_{max} and N_{min} correspond to the maximum and minimum coincidences $D_1 - D_{idler}$ as we vary the voltage on the piezoelectric device.

Visibility counts will vary as we change the difference in optical paths $\delta\phi$ by varying the voltage on the piezoelectric attached to the mirror, the idea is to see how visibility changes with voltage and keep the maximum value that we can achieve to keep going with the rest of the experiments.

DISCUTIR Y REDACTAR EL DE WHEELER CON BSs en chopper HAZ LAS FIGURAS(Correlaciones SPDC, SPDC tipo I) Y REVISAS LOS DEMAS COMENT-ARIOS

JUSTIFICAR LA BASE CON LA PAGINA 16 DE LA TESIS DE ZURI Y LOS APUNTES CON ALONSO

TAL VEZ ANADIR OPTICA NO LINEAL , CRISTALES Y TEORIA DE MEDI-CIONES EN APENDICES

ANADIR APENDICE DE CODIGOS

7 Conclusions

8   Appendices

References

[1] L. M. Procopio, O. Rosas-Ortiz, and V. Velázquez. On the geometry of spatial biphoton correlation in spontaneous parametric down conversion. *Mathematical Methods in the Applied Sciences*, 38(10):2053–2061, 2015.

[2] Z. Ou. *Multi-Photon Quantum Interference*. Springer US, 2007.

[3] R. Boyd. Nonlinear Optics - 3rd Edition.

[4] U. Leonhardt. *Essential Quantum Optics: From Quantum Measurements to Black Holes*. Cambridge University Press, 2010.

[5] G. Molina-Terriza, S. Minardi, Y. Deyanova, C. Osorio, M. Hendrych, and J. Torres. Control of the shape of the spatial mode function of photons generated in noncollinear spontaneous parametric down-conversion. *Phys. Rev. A*, 72:065802, Dec 2005.

[6] R. Chevalerias, Y. Latron, and C. Veret. Methods of interferometry applied to the visualization of flows in wind tunnels. *J. Opt. Soc. Am.*, 47(8):703–706, Aug 1957.

[7] P. Hariharan. *Basics of Interferometry*. Elsevier, Boston, October 1991.

[8] E. Ackerman. Broad-band linearization of a mach-zehnder electrooptic modulator. *IEEE Transactions on Microwave Theory and Techniques*, 47(12):2271–2279, 1999.

[9] P. Studenkov, M. Gokhale, W. Lin, I. Glesk, P. Prucnal, and S. Forrest. Monolithic integration of an all-optical mach-zehnder demultiplexer using an asymmetric twin-waveguide structure. *IEEE Photonics Technology Letters*, 13(6):600–602, 2001.

[10] J. Capmany and D. Novak. Microwave photonics combines two worlds. *Nature photonics*, 1(6):319, 2007.

[11] R. Loudon. *The Quantum Theory of Light*. OUP Oxford, Oxford ; New York, edición: 3 edition, November 2000.

[12] P. Knight and C. C. Gerry. *Introductory Quantum Optics*. Cambridge University Press, Cambridge, UK ; New York, edición: 1 edition, October 2004.

[13] L. Vaidman and A. C. Elitzur. Quantum mechanical interaction-free measurements. *L. Found Phys*, 23:987, (1993).

[14] Z. Blanco-García. Mediciones no destructivas en mecánica cuántica. M.Sc. Thesis(Advisors: O. Rosas-Ortiz , V. M. Velázquez) (2014).

[15] Z. Blanco-García and O. Rosas-Ortiz. Interaction-free measurements of optical semitransparent objects. *J.Phys.Conf.Ser.*, (2016) 01213.

[16] H. Azuma. Interaction-free measurement with an imperfect absorber. *Phys. Rev. A*, 74:054301, Nov 2006.

[17] P. Kwiat, H. Weinfurter, T. Herzog, A. Zeilinger, and M. A. Kasevich. Interaction-free measurement,. *Phys. Rev. Lett.*, 74:4763–4766, (1995).

[18] L.M. Procopio. Estudio teórico y experimental de la correlacion espacial de fotones como un primer paso al cómputo cuántico. M.Sc. Thesis(Advisors: O. Rosas-Ortiz , V. M. Velázquez) (2009).

[19] E. Hecht. *Optics*. Pearson, Boston, edición: 5th revised ed. edition, 2016.

[20] Krzysztof Wódkiewicz. Classical and quantum malus laws. *Phys. Rev. A*, 51:2785–2788, Apr 1995.

[21] U. Leonhardt. Quantum physics of simple optical instruments. *Reports on Progress in Physics*, 66(7):1207–1249, jun 2003.

[22] P. KWIAT, H. WEINFURTER, T. HERZOG, A. ZEILINGER, and M. KASEVICH. Experimental realization of interaction-free measurementsa. *Annals of the New York Academy of Sciences*, 755(1):383–393, 1995.

[23] B. Misra and E. C. G. Sudarshan. The zeno's paradox in quantum theory. *Journal of Mathematical Physics*, 18(4):756–763, 1977.

[24] R.J Glauber. Optical coherence and photon statistics. *Quantum Optics and Electronics*, 1, 1965.